We are IntechOpen, the world's leading publisher of Open Access books
Built by scientists, for scientists

6,900
Open access books available

185,000
International authors and editors

200M
Downloads

154
Countries delivered to

Our authors are among the

TOP 1%
most cited scientists

12.2%
Contributors from top 500 universities

BOOK CITATION INDEX
CLARIVATE ANALYTICS
INDEXED

WEB OF SCIENCE™

Selection of our books indexed in the Book Citation Index
in Web of Science™ Core Collection (BKCI)

Interested in publishing with us?
Contact book.department@intechopen.com

Numbers displayed above are based on latest data collected.
For more information visit www.intechopen.com

A Practical Guide to 3D Electromagnetic Software Tools

Guy A. E. Vandenbosch and Alexander Vasylchenko[1]
Katholieke Universiteit Leuven
Belgium

1. Introduction

This chapter considers the numerical analysis of planar antennas. First the fundamental theoretical techniques widely used in the general area of computational electromagnetics are discussed. The focus is on the specific case of planar antennas. Second, several simulation tools implementing these techniques are overviewed. Both commercial and non-commercial tools are considered. Examples found in literature are given. Third, three planar antennas are benchmarked, using a variety of tools, in order to show the reader the quality and matureness of the existing tools, and to prove that the analysis of planar antennas is by no means always straightforward. Remaining challenges that still need to be faced and "missing links" are identified, and suggestions are given for the future.

In the strictest sense a planar antenna means an antenna flat compared to the wavelength. Although the height of the antennas considered is different from traditional antennas, in most cases no special modeling techniques or software tools are used for planar antennas. Almost all planar antennas reported in literature have been designed / analyzed with the well-known techniques and (commercial) software packages. This means that in this chapter the major numerical techniques and software tools used can be overviewed in a general sense, referring to standard literature. These techniques will not be derived or explained here in detail. In stead, this chapter focuses on those aspects that come into the picture when the antenna is planar.

After the section on techniques and tools, this chapter will focus on the performance of these techniques and tools for planar antennas. This is done through an overview of benchmarks available in literature.

2. Modeling techniques

In this section the full wave solvers are introduced and categorized on the basis of their solution method: Integral Equations (IE) solved by Method of Moments (MoM), Finite Elements (FE), Finite Differences in the Time Domain (FDTD), and Finite Integration Technique (FIT). Based on their theoretical specificities, the application of each method in

---

the case of planar antennas is discussed. A history and a comprehensive overview of the different numerical techniques and of their application in computational electromagnetics (CEM) may be found in [1]. Recent work on the last developments in CEM [2] concentrates on the two main approaches of differential and integral methods. A Good review and perspectives concerning the relationship between differential and integral equations (IE) modeling is recommended in a review paper by Miller [3]. A thorough discussion on the different techniques with clarifying examples is also given in [4].

2.1 Integral equation techniques

Integral equation methods make use of Maxwell's equations in integral equation form to formulate the electromagnetic problem in terms of unknown currents flowing on the object to be described. The kernel of the integrals, or in other words the coupling between these currents and the fields, is formed by a Green's function tensor which includes the electromagnetic influence of the complete infinite so-called "background" environment, such that the problem formulation automatically covers the entire surrounding space without making any fundamental approximations. As a consequence, the corresponding solution is automatically valid in every point of the background medium. Far field radiation phenomena, surface waves in layered structures, etc., that are vital for efficient and accurate antenna analysis, are analytically included in the solution.

By straightforward application of the classic Method of Moments (MoM), as introduced in the basic book [5], boundary equations expressing the physical nature of the object to be described (conductivity on a conductor, permittivity in a dielectric part of the object), are enforced. This is either done at the boundaries of volumes utilizing Surface Integral Equations (SIE) [6] or inside the entire volumes themselves, applying Volume Integral Equations (VIE) [7] on the inside of the components. IE-MoM gives rise to a dense matrix equation, which can be solved using standard matrix algebra technology.

IE-MoM is normally applied in the frequency domain, i.e. for time-harmonic problems. This means that the solution has to be determined at each frequency of interest.

Intrinsically, IE formulations are very powerful, since they inherently minimize the number of unknowns for a certain problem. IE can be formulated also very general. Volumetric MoM for example in principle can describe any arbitrary structure, involving the most complex features. However, the resulting dense MoM matrix invokes a large memory demand. Also, there is a lack of matrix solvers comparable in efficiency to the solvers used in the differential equation techniques, which yield sparse matrices. This has precluded the use of volumetric MoM for modeling complex structures on widespread computer systems.

In general, it can be stated that state-of-the-art IE-MoM-based solvers are more efficient for open region problems, possibly involving multiple layers, involving impenetrable or homogeneous objects, since IE-MoM satisfies the radiation condition automatically through the Green's function.

It has to be noted that the integral equations can be written down in different forms (dyadic form, mixed-potential form, hybrid forms, etc. [8]), which give rise to specific implementations, as found in the different commercial solvers.

In the following sections, several aspects linked with the use of integral equation techniques for planar antennas are discussed.

2.1.1 Occurrence of layer structures

As explained above, IE technique solvers are formulated making use of Green's functions. These Green's functions can be formulated for multi-layered structures, such that the

background medium of the antenna may consist of an arbitrary number of horizontal, infinitely stretched, dielectric and metallic layers, which are taken into account analytically. This environment is particularly interesting for the numerous families of planar antennas and circuitry designs, because the horizontally large components such as dielectric substrates or conducting ground planes can be contained in the environment. The only remaining components are local scattering objects with medium or small dimensions such as radiating patches, apertures, or volumetric inhomogeneities. These components are replaced with equivalent surface/volume currents, which appear as the primary unknowns in the resulting integral equations.

However, in many planar antennas extended layer structures do not occur, and the computational advantages linked to the use of IE for this type of structure in many cases simply are irrelevant. Only in cases where planar antennas are used for example on larger PCB structures, the PCB substrate may be modeled efficiently by IE-MoM [9]. Nevertheless, even then, in the benchmarking section, it will be shown that solvers based on IE techniques are in many cases still very fast.

2.1.2 Complex environment

In case the environment is really complex, with inhomogeneous lossy dielectrics (e.g. biological tissue, [10]), the IE-MoM technique is inferior to the differential equation techniques discussed in the next section. The reason is that, in case a pure IE-MoM technique is used, the inhomogeneity of the dielectrics of the environment has to be described by Volume Integral Equations, leading to a number of unknowns proportional to the size of the volume of the object + environment. Even if the number of unknowns in these cases is still below the number of unknowns for differential equation techniques, the dense coupling matrix of the IE-MoM technique requires much higher computational resources and in practice prohibits its use.

This drawback may be partially overcome by developing special techniques, taking into account the specificities of different regions [11], but their implementation and application in the case of planar antennas is still in its infancy.

2.2 Differential equation techniques

Differential equation methods are derived directly from Maxwell's curl equations or the Helmholtz wave equations with little analytical preprocessing. The most popular differential equation-based methods are the Finite Element Method (FEM), for example utilized in Ansoft's HFSS software package, and the Finite-Difference Time Domain method (FDTD), which is employed for example by CST's Time Domain transient solver (in the particular case of Cartesian grids).

Since the number of unknowns is proportional to the volume and the resolution considered, differential equation methods are particularly suitable for modeling small full three-dimensional volumes that have complex geometrical details, for example smaller closed-region problems involving inhomogeneous media [12]. Intrinsically, differential equations are less suited for open problems. The reason is that in principle they require a discretization of the entire space under consideration. This space is limited in case of closed problems, but corresponds to infinite space in case of open problems. In practice, this problem is solved by the introduction of techniques like Absorbing Boundary Conditions, and Perfectly Matched Layers (PML) [13]. The quality of these truncating techniques nowadays is so high that, in practice, this fundamental problem has been overcome, albeit it in an approximate numerical way.

Since many techniques to make planar antennas small involve complex topological 3D shaping, the use of non-homogeneous dielectrics, etc., differential equation techniques have a clear inherent advantage for these structures over integral equation techniques.

2.2.1 The Finite Element Method (FEM) [13], [14]

FEM is a method based on solving partial differential equations. It is most commonly formulated based on a variational expression. It subdivides space in elements, for example tetrahedra. Fields inside these elements are expressed in terms of a number of basic functions, for example polynomials. These expressions are inserted into the functional of the equations, and the variation of the functional is made zero. This yields a matrix eigenvalue equation whose solution yields the fields at the nodes.

Its first formulations were developed as matrix methods for structural mechanics. This lead to the idea to approximate solids and Courant (1942) introduced an assembly of triangular elements and the minimum of potential energy to torsion problems [15]. The first paper on the application of FEM to electrical problems appeared in 1968 [16]. An extensive review on the history of FEM in electromagnetics was published in an issue of the Antennas and Propagation Magazine [17]. FEM normally is formulated in the frequency domain, i.e. for time-harmonic problems. This means that, as for IE-MoM, the solution has to be calculated for every frequency of interest.

Numerous references can be given developing, explaining, and using FEM. A good book to start with is [14]. A software tool using FEM and very widely spread is Ansoft HFSS.

2.2.2 The Finite-Difference Time-Domain technique (FDTD) [18], [19], [20]

The nature of Maxwell's differential equations is that the time derivative of the H-field is dependent on the curl of the E-field, and the time derivative of the H-field is dependent on the curl of the E-field. These basic properties result in the core FDTD time-stepping relation that, at any point in space, an updated value of an E/H-field in time is dependent on the stored value of the E/H-field and the numerical curl of the local distribution of the H/E-field in space. The numerical translation into a time-stepping algorithm was introduced by Yee in 1966. Indeed, swapping between E-field and H-field updates allows to define a marching-on-in-time process wherein sampled fields of the continuous electromagnetic waves under consideration are used. These waves can be seen to propagate in the Yee lattice, a numerical three-dimensional space lattice comprised of a multiplicity of Yee cells. More specifically, Yee proposed a leapfrog scheme for marching-on in time wherein the E-field and H-field updates are staggered so that E-field updates are observed midway during each time-step between successive H-field updates, and vice versa. Positive is that this explicit time-stepping scheme avoids the need to solve simultaneous equations. It also yields dissipation-free numerical wave propagation. Negative is that this scheme results in an upper bound on the time-step to ensure numerical stability. This means that simulations may require many thousands of time-steps for completion. The use of the Yee lattice has proven to be very robust in numerical calculations.

FDTD is extremely versatile since the interaction of an electromagnetic wave with matter can be mapped into the space lattice by assigning appropriate values of permittivity to each electric field component, and permeability to each magnetic field component. This can be done without seriously compromising the speed of the method.

The fact that time is observed directly, and the versatility of the method, make it the most efficient technique for complex 3D transient problems. A very efficient implementation of the FDTD technique can be found in the commercial tool Empire [21].
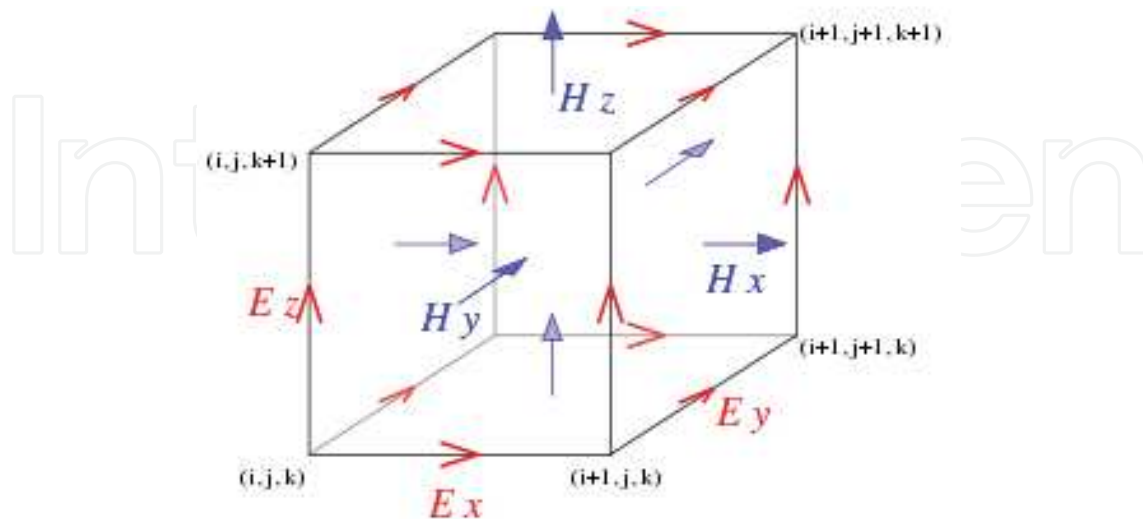

Fig. 1. Standard Cartesian Yee cell used in the FDTD technique.

2.2.2 The Transmission Line Matrix method (TLM) [22]

The TLM method is a special Finite-Difference Time-Domain technique. It is based on elementary parallelepiped cells obtained with an interconnected transmission lines network. The propagation and scattering of voltage impulses through this network is equivalent to the propagation of electromagnetic fields in arbitrary media. At each time step, a scattering matrix associated to each cell computes the reflected voltage impulses from the incident ones. This reflected voltage impulses become incident voltage impulses on the six neighboring nodes for the next time step. The six electromagnetic fields are directly related to the incident voltage impulses at the center of the cell. Capacitive, inductive and resistive stubs connected to the nodes allow to take into account variable cell sizes, permittivity, permeability, electric and magnetic conductivities. Free space is simulated by using a modified TLM node allowing implementation of PML.

2.2.2 The Finite Integration Technique (FIT) [23]

The Finite Integration Technique was introduced by Weiland in 1977. The word integration does not imply any relation with integral equations. FIT first describes Maxwell's equations on a grid space. The matrix equations for the electromagnetic integral quantities obtained by FIT possess some inherent properties of Maxwell's equations, for example with respect to charge and energy conservation. This makes them very attractive from a theoretical point of view. FIT can be formulated on different kinds of grids, e.g. Cartesian or general non-orthogonal ones, which is a clear advantage. In the time-domain, which is our field of interest, the resulting discrete grid equations of FIT are, at least in "some" cases, identical to the discrete equations derived with the classical Finite-Difference Time-Domain (FDTD) method. In contrast to FIT, which is applied to the integral form of the field equations, FDTD (as a subset of the finite integration method) is applied to the differential form of the governing Maxwell curl equations. Theoretical links between FDTD and the FIT approach realized in CST may be

found in [24]. A comparative study on Time Domain methods was presented in [25]. In some sense, FIT can thus be considered as a powerful generalization of the FDTD technique. A software tool using FIT and very widely spread is CST Microwave Studio.

3. Software tools

In the following sections, several solvers are briefly described with more specific information on the implemented solution method. Commercial solvers and academic solvers are considered. For some of the commercial solvers an application section is given, where references to literature can be found. In these papers designs based on these solvers are reported. It has to be emphasized that by no means this overview is complete. The references given are just mere illustrations. A wealth of information concerning this issue can be found in the IEEE Antennas and Wireless propagation Letters, where over the years numerous designs of planar and integrated antennas can be found.

3.1 Commercial software tools

Since the cost of a commercial solver in many cases is high, the choice of the commercial solvers considered was based on their availability to the authors, directly or through cooperation with others. The fact that a specific solver is missing does not represent any statement about its quality. Nevertheless, the authors believe that the solvers selected do represent the global landscape in this area.

The IE solvers are roughly ordered according to increasing complexity of the geometries that can be handled and in addition to that, meshing abilities are clarified for every software package.

3.1.1 Momentum [26]: IE-MoM

HP-Momentum is the IE-MoM solver integrated within the ADS system of Agilent. The integral equations are formulated in mixed potential form and the matrix elements are evaluated completely in the spatial domain. Momentum was originally developed to analyze planar circuitry. The latest version of Momentum can model vertical currents per layer as well as horizontal side-currents on thick conductors. A combination of rectangles and triangles represent cells of Momentum's mesh grid. The mesh reduction option allows the shape of basis functions to incorporate some of the physics of the design and the mesh cell can be any polygon compounded by rectangles and triangles. Nevertheless, the modeling of finite dielectric volumes is not included, which limits the modeling capabilities for full 3D structures. These limitations can be resolved by running EMDS (the FE based solver included into the ADS package) without having to run a stand-alone tool. Mesh frequency and number of cells per wavelength are used for determining the mesh density of the entire circuit or any single object. The edge meshing option adds a relatively dense mesh along the edges of objects. Since the current density is higher along the edges of objects, the edge mesh can improve the accuracy and speed of a simulation.

3.1.2 IE3D [27]: IE-MoM

The integral equations are formulated with a full dyadic Green's function and the matrix elements are computed completely numerical in the spatial domain. IE3D can model truly arbitrary 3D metal structures. Since 2006 also finite 3D dielectric volumes can be modeled with a VIE approach (Volume Integral Equation). IE3D performs automatic generation of a

non-uniform mesh with both rectangular and triangular cells. The user can control the highest meshing frequency and the number of cells per wavelength. An automatic edge cell feature is available for accurate simulation of the currents concentrated near the edges of metallic surfaces.

IE3D has been successfully used in the design of small antennas for mobile phones. Specific topologies can be found in [28], [29], [30], [31], [32]. In [30] for example, an internal dual-band patch antenna is described. The antenna is simulated and measured and the agreement is excellent for this topology. An external multi-band antenna can be found in [33]. In general, impedance, radiation patterns, and radiation efficiency seem to be well predicted.

3.1.3 FEKO [34]: IE-MoM, in combination with other techniques

FEKO is based on the IE-MoM method, which can be combined with other techniques, like the geometric optics approach (GO), the unified theory of diffraction (UTD), and the multilevel fast multimode method (MLFMM). GO and UTD are at the moment the only practical approaches for solving a class of very large problems, the size of which exceeds the handling capabilities of MoM, FEM or FDTD [35]. The matrix elements are computed using a mixed-potential formulation and a spatial domain approach. The solver can model truly arbitrary 3D structures. Dielectric volumes can be modeled in three different ways: with a SIE approach, with a VIE approach, or with a hybrid approach with the FE method. The surface of the structure is discretized using a triangular mesh, while tetrahedra are used for volumetric discretization. In order to allow flexible control of the mesh, a user can specify different cell dimensions for any selected region, face or edge.

3.1.4 HFSS [36]: FEM

Since it was one of the first tools in the market, and also due to its generality and flexibility, HFFS is one of the tools heavily used in industrial design environments. The purpose of HFSS is to extract parasitic parameters (S, Y, Z), visualize 3D electromagnetic fields (near- and far-field), and generate SPICE models, all based on a 3D FEM solution of the electromagnetic topology under consideration. Very useful features of HFSS are its automatic adaptive mesh generation and refinement, which in most cases frees the designer of worrying about which mesh/grid to choose.

This software is extremely popular and is used for all kinds of purposes. Specific results for small planar antenna topologies can be found in [37], [38], [39], [40], [41], [42]. Input impedance and radiation patterns are generally predicted very well. Few results are found about the efficiency.

3.1.5 Empire [21]: FDTD

Empire XCcel is based on the FDTD technique. Due to adaptive on-the-fly code generation it comes with a highly accelerated kernel, providing very fast simulations. It features the Perfect Geometry Approximation (PGA) algorithm to yield more accurate results for curved structures, frequency dependent loss calculation and special algorithms for modeling thin conducting sheets. Several structure import and export formats are supported. EMPIRE XCcel's applicability ranges from analyzing planar, multi-layered and conformal circuits, components and antennas to multi-pin packages, waveguides, and SI/EMC problems including the device's operational environment. Time signals, scattering parameters, and field animations are generated for a broad frequency range within only one simulation run.

Monitoring and animation capabilities give physical insight into electromagnetic wave phenomena while accurate results are obtained with little effort.

3.1.6 CST [43]: FIT

CST Microwave Studio (CST MWS) is based on the finite integration technique (FIT). It allows to choose the time domain as well as the frequency domain approach. Despite the presence of transient, eigenmode, and frequency domain solvers within CST MWS, the transient solver was examined for benchmarking further in this chapter as the flag ship module of CST MWS. The Time Domain Solver calculates the broadband behavior of electromagnetic devices in one simulation run with an arbitrarily fine frequency resolution. The modeling of curved structures using the Perfect Boundary Approximation® technique and the modeling of thin perfectly electric conducting sheets with the Thin Sheet Technique® tries to cope with the typical difficulties inherent to classical FDTD methods. The transient analysis of the proposed antennas is done utilizing the hexahedral mesh type. The automatic mesh generator detects the important points inside the structure (fixpoints) and locates mesh nodes there. The user can manually add fixpoints on a structure, as well as fully control the number of mesh lines in each coordinate with regards to the specified wavelength. Energy based adaptation of the mesh allows to refine it in a predefined number of passes, providing a mesh refinement of sophisticated design features for the price of longer overall simulation time. The analyses in this chapter use automatic direct meshing without any local settings. Although the FIT in principle can handle material parameters changing over the dielectric volumes defined, this is not implemented yet.

CST, as a general purpose software package being a real competitor for HFSS, has gained popularity in the last few years. Also for the analysis and design of planar and small antennas, more and more results obtained with CST can be found in literature, for example in [70]. A problem sometimes observed with CST is a ripple in the frequency response in case the tool settings are not appropriate. This is due to the fact that the flagship of CST is inherently a time domain solver.

3.2 Non-commercial software tools
3.2.1 MAGMAS 3D [44], [45] [46], and [47]: IE-MoM

MAGMAS 3D is the IE-MoM code developed at the Katholieke Universiteit Leuven, Belgium. It was developed in cooperation with the European Space Agency for 2D, 2.5D and quasi-3D structures. Specific in comparison with other MoM codes is that the matrix elements are computed using a hybrid dyadic-mixed potential formulation and a combined spectral-space domain approach. This allows to perform a large part of the computation procedure for these matrix elements analytically in the spectral domain. This makes the code computationally more efficient. Surface and volume currents are decomposed in horizontal and vertical currents (= quasi 3D approximation), which are both expanded using generalized rooftop functions. A full mesh control of combined rectangular and triangular mesh cells is available in manual meshing mode. Exact coordinates and dimensions can be set for every single mesh cell. A Graphical User Interface is available.

4. Benchmarking

Nowadays, antenna engineers rely heavily on highly specialized full wave electromagnetic (EM) field solvers to develop and optimize their designs. Computer-aided analysis and

optimization have replaced the design process of iterative experimental modifications of the initial design [48]. The operation of these EM solvers is based on the numerical solution of Maxwell's equations in differential or integral form. It is evident that the underlying solution method significantly influences the efficiency and accuracy by which certain structure types are analyzed. Nevertheless, the commercial focus increasingly switches from such key theoretical considerations to improvements in the area of layout tools and system-level design tools. Therefore, users may get the wrong impression that a given solver is automatically suited to solve any kind of problem with arbitrary precision. This is of course not true.

This section verifies the plausibility of such expectations by presenting an extensive benchmark study for planar antennas which focuses on the capabilities and limitations of the applied EM modeling theories that usually remain hidden for the antenna designer. Many challenging problems for EM solvers, which turn on the fundamental capabilities of modeling techniques, were highlighted in papers in open literature [49].

To ensure a well-founded result, the scope of the investigation is extensive: different commercial packages and a home-made academic solver are used to analyze very different but characteristic planar antenna structures, which are subsequently manufactured and measured. This work also leads to establishing guiding rules to assist users in choosing the appropriate simulation software for a specific antenna design. It is important to note that only theoretical considerations will be taken into account: the benchmark study does not include the comparison of Graphical User Interfaces (GUI), price/performance ratio, user friendliness, etc.

To our knowledge, such an extensive benchmark study over a large variety of solvers and for several structures was only reported in [50], which is the core paper providing most of the basic material for this section. In [51] and [52] a comparable analysis was conducted using four different solvers, but only for one structure. An accuracy and speed benchmark on six EM solvers was presented in [53] for four different antennas, but the physical link between simulation results for a specific antenna problem and the applied solution method has not yet been generally established. [54] and [55] present comparison of commercial EM solvers with measurements in predicting S-parameters for resonating structures.

Each method described above is represented in the benchmark by at least one widely known commercial solver. Due to the much higher level of analytical pre-processing for the IE-MoM solvers, they show a huge range of possibly implemented algorithms. That is why in this benchmark the differential solvers (FE and FDTD) are outnumbered by the IE-MoM solvers.

Since commercial solvers are often very expensive, although they are often available with substantial discounts to academic institutions, their availability is limited. Apart from the academic solver MAGMAS 3D, the other IE solvers included in this benchmark are IE3D of Zeland Software, FEKO of EM Software & Systems, and ADS Momentum of Agilent. Three of the leading differential EM tools: HFSS of Ansoft for the FE method, Empire and CST Microwave Studio for the FDTD method were also introduced. Good reviews of these CEM techniques and solvers may be found in [56]. The versions used for the respective software tools are given in Table 6.

4.1 Antenna structures
4.1.1 Line fed planar patch with local dielectric inhomogeneity
The antenna depicted in Fig. 2 is ideally suited to serve as a first reference benchmark structure. It is a classical, well-known structure. It is the basis for many small planar antennas on which to apply a single or a combination of miniaturizing techniques (PIFA, S and E antenna, H antenna, patches with slots, etc.). It contains elements that are naturally unsuited for both the differential and the integral equation solver families.

The structure consists of a line-fed patch antenna, situated on an infinitely stretched, grounded dielectric substrate of thickness d = 1.52 mm and permittivity ε = (3.38 - j0.0074) ε_0. A local dielectric inhomogeneity with permittivity ε_d is added to the infinitely stretched substrate in the form of a finite dielectric volume under the patch. Such modifications to the substrate structure can be used to improve the radiation pattern [57], to control the surface wave coupling with other elements [58], or to miniaturize the patch. The square patch (W = L = 15.2 mm, H = 5.07 mm) is symmetrically fed by a simple microstrip line of which the dimensions L_1 = 30.4 mm, L_2 = 5.7 mm and W_s = 3.8 mm are indicated in Fig. 2.

The antenna is analyzed on a completely homogeneous substrate, i.e. for ε_d = ε = (3.38 - j0.0074) ε_0, and also analyzed on an inhomogeneous substrate, with a dielectric volume of ε_d = (3.00 - j0.0039)ε_0 included under the patch.
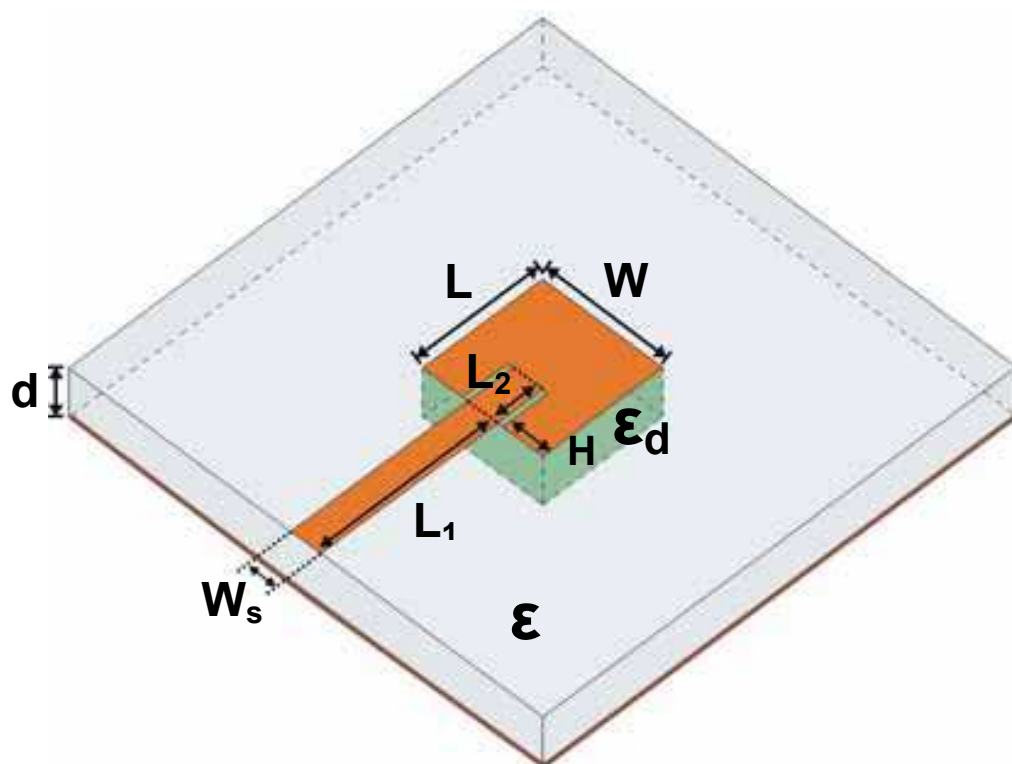
Fig. 2. Line-fed patch antenna on an inhomogeneous substrate.

4.1.2 UWB antenna

Small-size, low-cost planar UWB antennas have recently received considerable interest due to the new release of the frequency band from 3.1 to 10.6 GHz for short-range low-power communication. The Printed Tapered Monopole Antenna (PTMA), see Fig. 3, is a typical representative of contemporary UWB designs [59]. The structure with maximum dimensions of 25.0 x 28.5 x 1.27 mm^3 (w x l x h) consists of a tapered radiating element fed by a microstrip line. In order to obtain broad band behavior two slots are added in the radiating element and in the ground plane, respectively. All metal parts are simulated as perfect electric conductors. The antenna prototype was etched on a piece of PCB (RO3210) with ε_p = 10.2 (tanδ=0.0027). The dimensions are: W_{UWB} = 24 mm, L_{UWB} = 20 mm, S= 1 mm, l_a = 18 mm, and w_t = 4 mm. Fig. 4 shows the configuration of the microstrip feeding with W_f = 2 mm, W_m =3 mm, L_{m1} = L_{m2} = 4 mm, W_c = 4 mm, L_c = 4 mm, and L_{gr} = 8 mm. The UWB

antenna topology has a symmetrical design. Hence, a symmetry plane can be defined, in order to reduce the simulation time.
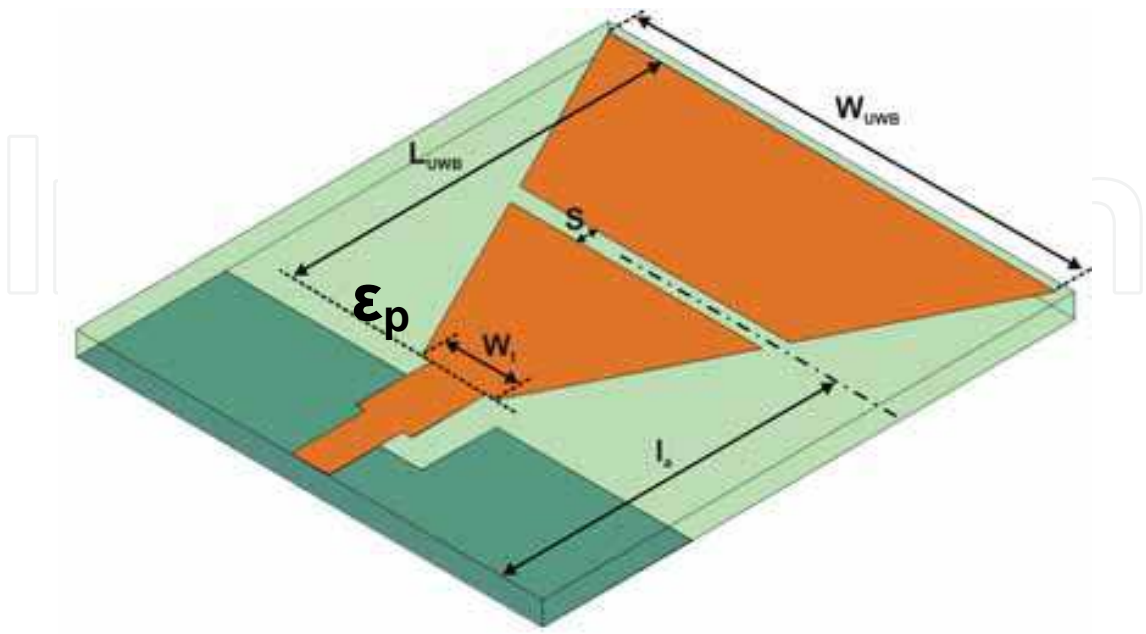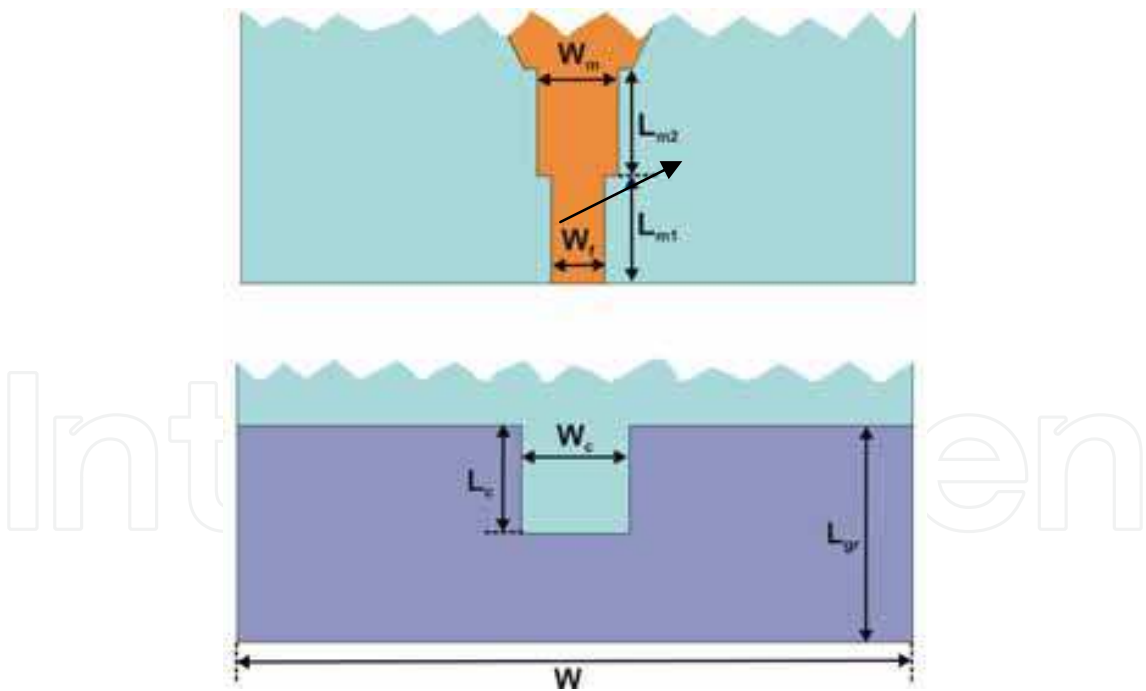

Fig. 3. UWB monopole antenna topology.

Fig. 4. UWB monopole antenna feeding system, top and bottom view.

4.1.3 Folded monopole antenna for GSM application

The RangeStar Ultima™ 'World GSM antenna' (P/N 100709), covering the three GSM frequency bands, is an example of a planar monopole antenna. Its specifications indicate a 2.5:1 VSWR in the frequency bands 880–960 MHz and 1710–1990 MHz. The substrate is

assumed to be a typical PCB material such as FR4, with dielectric permittivity ε_g = 4.4 and tanδ=0.02. An integrated planar test version of this antenna using monopoles, ground plane and coplanar feeding line printed on the same interface was manufactured. The test PCB has outer dimensions 37.6 x 46.275 mm². The substrate thickness is d = 1.57 mm. A sketch of the full topology is given in Fig. 5. The antenna (represented in orange) with the outer dimensions 36.88 x 9.42 mm² (W_{GSM} x L_{GSM}) is fed in the center. The feeding CPW conductor, which is separated from the pair of ground planes (15.2 x 32.2 mm² (W_{GP1} x L_{GP}) for GP1, and 19.541 x 32.2 mm² (W_{GP2} x L_{GP}) for GP2) with S = 0.218 mm width for the slots, has W_s = 1.7 mm width. The left-hand part is a short monopole which mainly resonates in the upper frequency band, while the right-hand part is longer and resonates in the lower frequency band. On the lower right of the antenna there is a short circuit to match the antenna to a 50 Ω feed. The antenna is at a distance G = 2.2 mm from the ground planes.
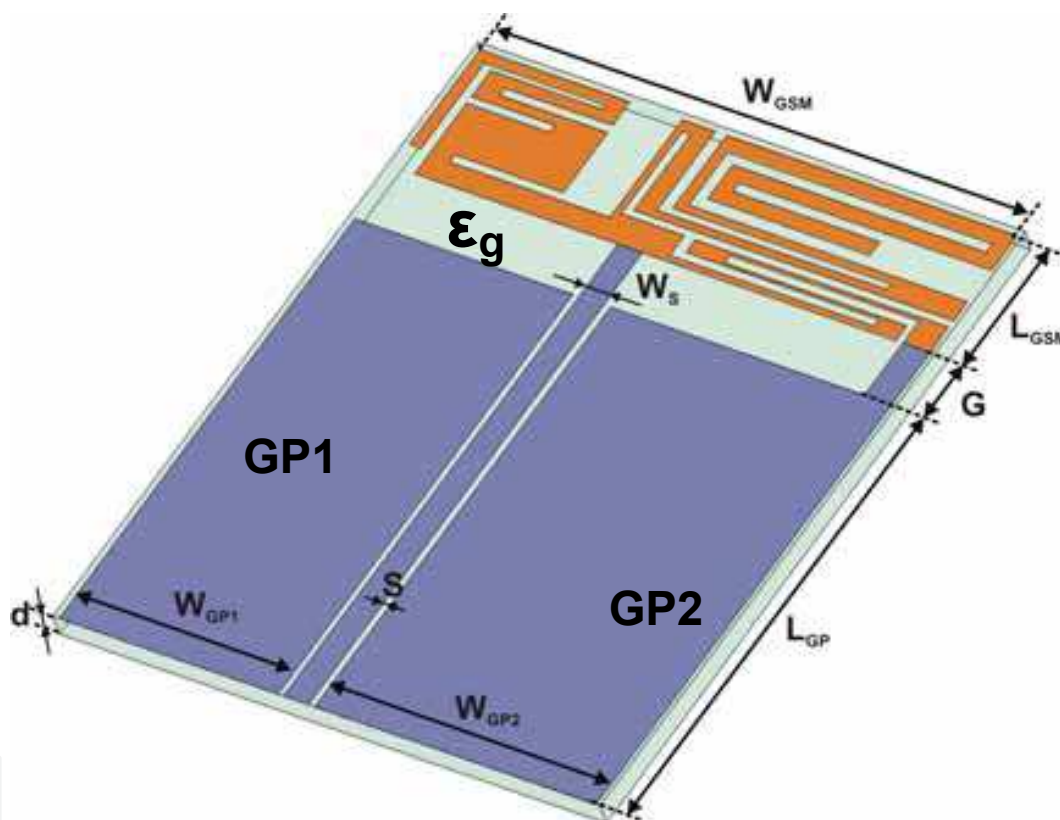

Fig. 5. CPW-fed GSM antenna integrated on a test PCB.

4.2 Measurement setup

The antennas were fabricated, see a photo in Fig. 6, and measured. A 50 Ω SMA was connected to the end of the feeding strip/probe and grounded to the ground plane. An RF cable from the Vector Network Analyzer (HP85107B) was connected to the SMA to excite the Antenna Under Test (AUT). It is well-known that the measurement of a small planar antenna is very sensitive to the presence of the RF cable located in the near field of the AUT [60]. The additional radiation from the outer surface of the signal cable can have a significant impact on the measured parameters such as operating frequency, radiation pattern, and gain. Ferrite chokes around the front end of the cable were used to reduce the additional radiation from the signal cable by forming a high impedance, in this way reducing the current on the outer cable surface [61].

Since our point of interest is the return loss only, during the measurements an anechoic box was used in order to suppress the influence of any metallic object in the surroundings. The box has a cubical form with an edge size of 80 cm and the inner faces are covered with the absorbing material HR-05 from Emerson & Coming, with absorber length 610 mm. These absorbers do not reveal any measurable effect on the radiation characteristics of the electrically small patch antenna around 1.8 GHz, as long as they are kept further than 100 mm away from the AUT [62]. Every AUT was put into the middle of the anechoic box and hung there by the RF cable only. Thus, the distortions in the measurement of the S11 parameter were minimized due to the absence of any unnecessary object in the near field of the AUT.
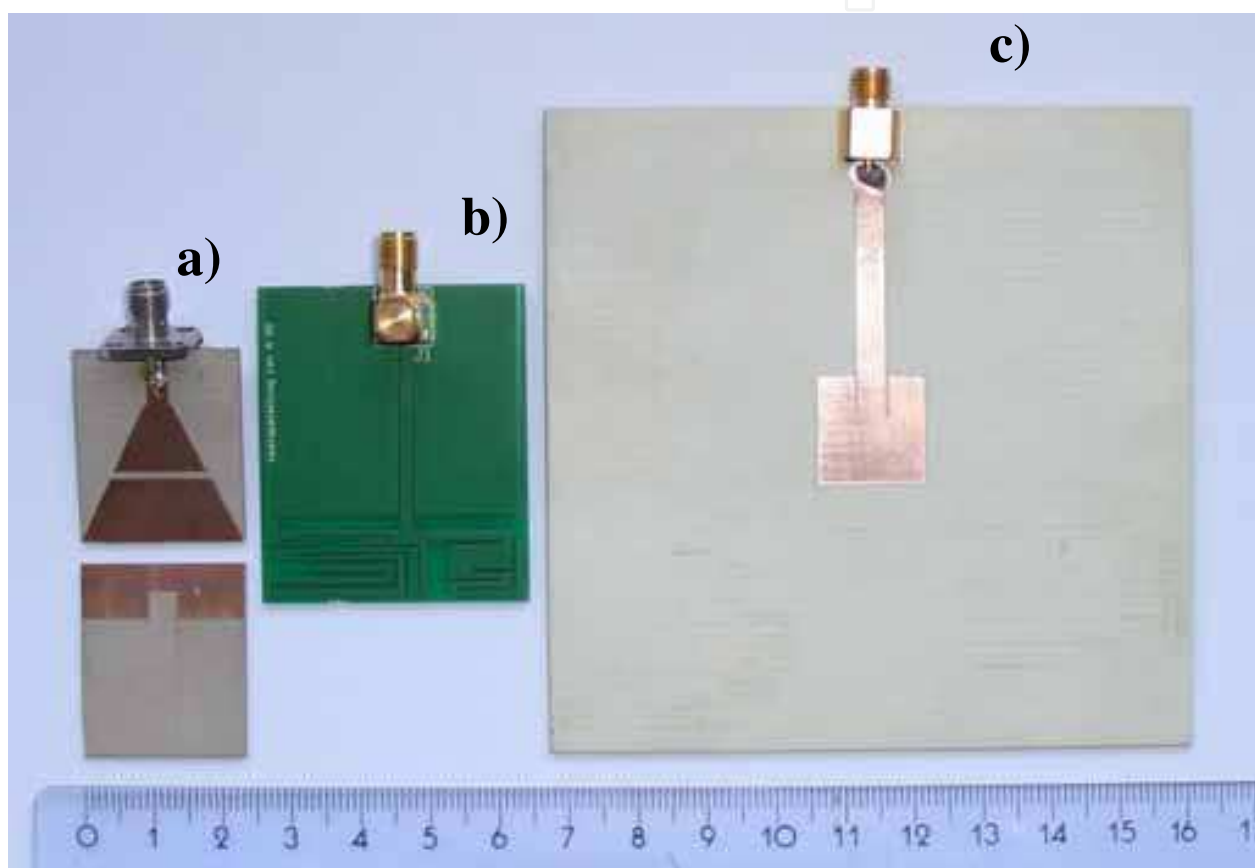

Fig. 6. Antenna prototypes: a) UWB monopole (top and bottom view); b) GSM RangeStar UltimaTM integrated on test-PCB with ground plane; c) line-fed patch on the homogeneous substrate.

4.3 Benchmarking results
4.3.1 Line fed patch antenna
The line-fed patch antenna is first simulated for a completely homogeneous substrate with $\varepsilon = (3.38 - j0.0074)\, \varepsilon_0$. For the solvers MAGMAS 3D, IE3D, FEKO and MOMENTUM, the homogeneous substrate is modeled as an infinitely stretched dielectric layer and included as such in the background. This implies that only the metallic parts give rise to unknowns. In MAGMAS 3D, IE3D and MOMENTUM, the stripline feed is modeled by a horizontal port

model which assumes an incident voltage wave arriving from infinity. In a second analysis the dielectric inhomogeneity is included as a volume with permittivity $\varepsilon_d = (3.00 - j0.0039)\,\varepsilon_0$ and dimensions $15.2 \times 15.2 \times 1.52$ mm³. This volume is described by unknown polarization currents. Only MAGMAS 3D and IE3D can calculate Green's functions for layered media with discretization of only a small dielectric volume with permittivity different from the host medium. A multilayer substrate and dielectric bodies cannot be combined in FEKO. Therefore, FEKO models the patch on the inhomogeneous substrate using free-space Green's functions with discretized finite volumes for both dielectrics. This volumetric discretization of both dielectrics dramatically increases the number of unknowns of the whole problem and significantly rises its computational time. Since finite dielectric volumes are not supported by MOMENTUM, it is impossible to simulate the patch antenna on the inhomogeneous substrate.

In order to be able to look at the simulation results in a wider perspective, the two antenna designs were realized and measured (Fig. 7). The homogeneous antenna (Fig. 6c) was realized simply by mechanically etching the required metallic shape on the RO4003 substrate. The fabrication of the inhomogeneous design was somewhat more involved. The feeding line was etched on the RO4003 substrate with a square hole spared out at the position of the patch. An equally sized piece of RO3003 substrate, with only the insets of the patch etched out, was then fitted into the hole to construct the antenna. The electrical conductivity was ensured by soldering the metal junctions. The strip lines are fed by a straight coaxial PCB connector of Huber & Suhner: type SMA-S50-0-45, mounted at the edge of the substrate.
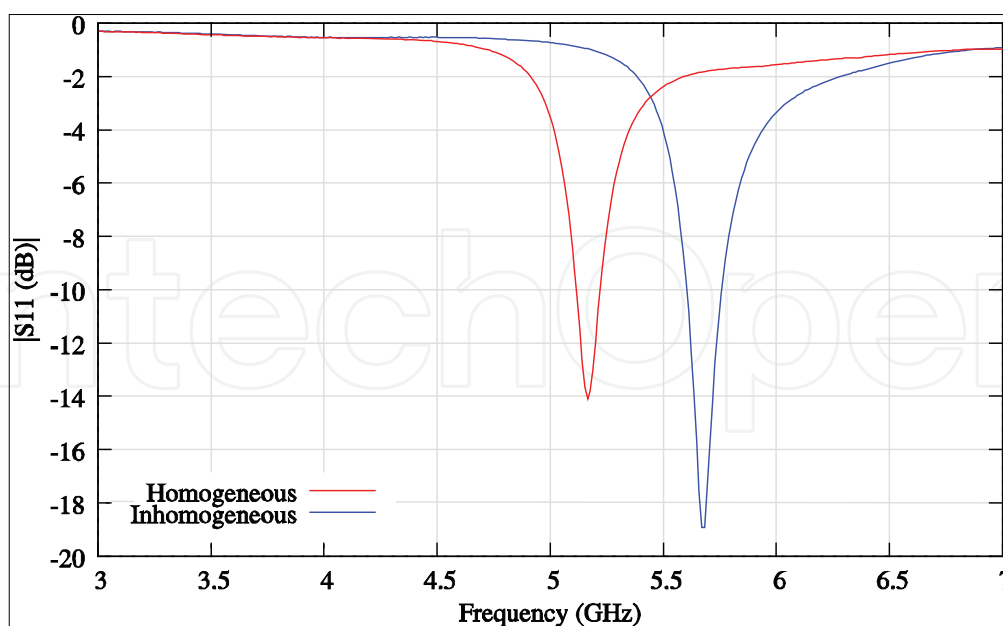

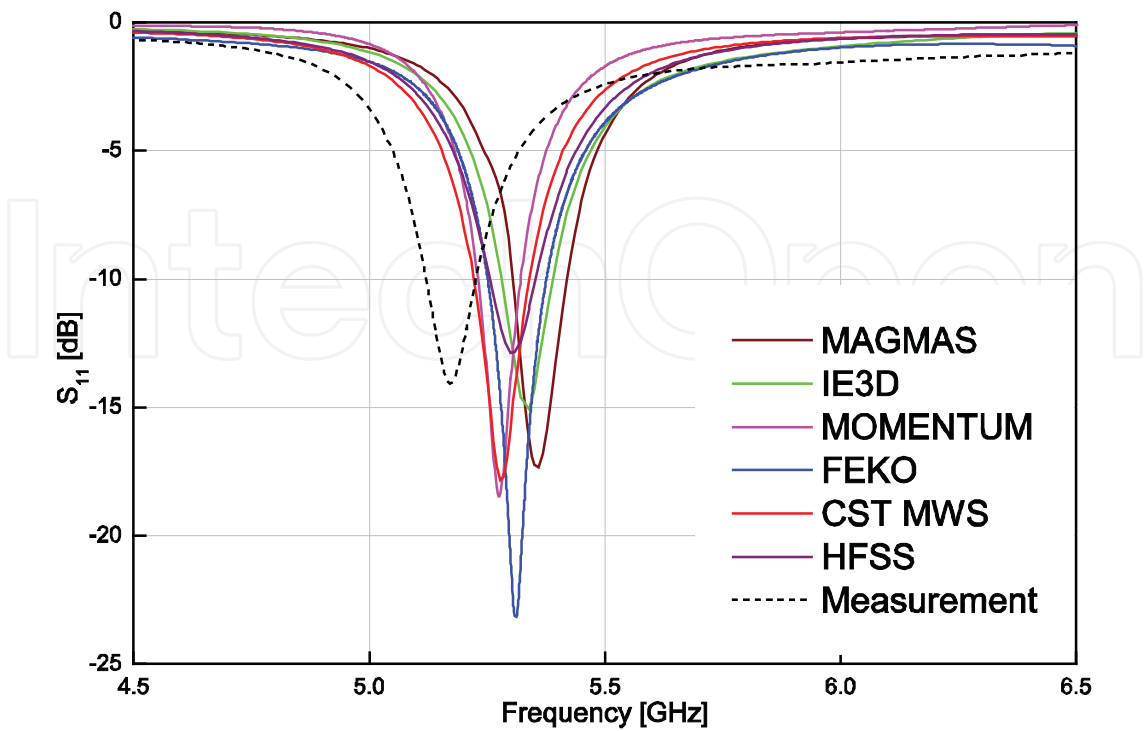Fig. 7. Measurement for line-fed patch on homogeneous and inhomogeneous substrate.
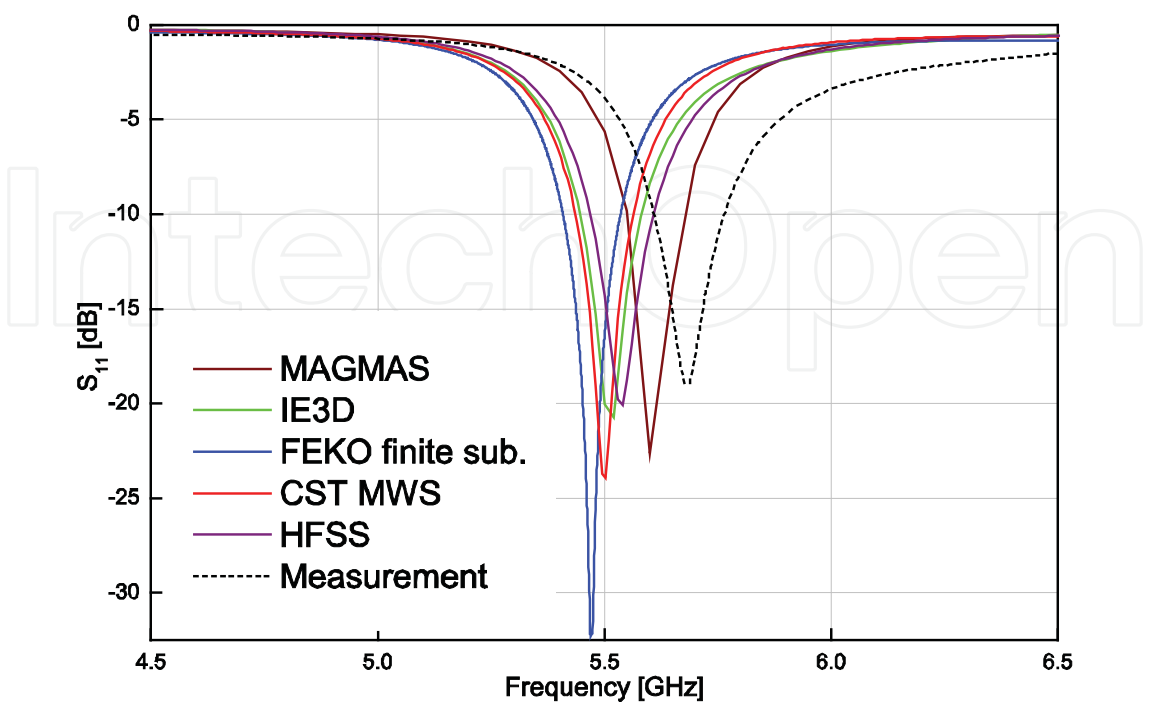
Fig. 8. Simulations and measurements for line-fed patch antenna on homogeneous substrate.

Software Package	Fmin (GHz)	Fmax (GHz)	Fc (GHz)	Fc-shift (%)	BW (GHz)	FcD (%)
MAGMAS	5.305	5.421	5.363	3.67	0.116	0.96
IE3D	5.28	5.39	5.335	3.13	0.11	0.44
FEKO	5.25	5.375	5.313	2.7	0.125	0.01
MOMENTUM	5.23	5.321	5.276	1.98	0.091	-0.68
HFSS	5.256	5.353	5.305	2.54	0.097	-0.14
CST MWS	5.22	5.34	5.28	2.07	0.12	-0.60
Measurement	5.12	5.226	5.173	0.0	0.106	-2.61

Table 1. Nominal frequency values for patch antenna on homogeneous substrate at return loss level of -10 dB.

Fig. 9. Simulations and measurements for line-fed patch antenna on inhomogeneous substrate.

Software Package	Fmin (GHz)	Fmax (GHz)	Fc (GHz)	Fc-shift (%)	BW (GHz)	FcD (%)
MAGMAS	5.55	5.68	5.615	-1.25	0.13	1.58
IE3D	5.445	5.581	5.513	-3.04	0.136	-0.26
FEKO	5.408	5.535	5.472	-3.77	0.127	-1.01
MOMENTUM	NA	NA	NA	NA	NA	NA
HFSS	5.47	5.608	5.539	-2.59	0.138	0.21
CST MWS	5.435	5.563	5.499	-3.29	0.128	-0.52
Measurement	5.61	5.762	5.686	0.0	0.152	2.87

Table 2. Nominal frequency values for patch antenna on inhomogeneous substrate at return Loss level of -10 dB.

The simulation results in Fig. 8 and 9 show S_{11} from 4.5 to 6.5 GHz. Tables 1 and 2 give the data in absolute values. The minimal and maximal frequencies crossing the Return Loss level at -10 dB are Fmin and Fmax respectively. The difference between Fmin and Fmax defines the bandwidth (BW) at S11 = -10 dB. The central frequency (Fc) is determined by Fc = (Fmax + Fmin)/2. Hence, the Fc-shift is the deviation between Fc measured and Fc simulated. The central frequency deviation (FcD) shows the dispersion with respect to the mean of the simulated results only. It has the purpose to exclude fabrication and measurement inaccuracies. It is defined as FcD = Fc – FcAV, where

$$FcAV = \frac{1}{n}\sum_{i=1}^{n}Fc \tag{1}$$

is the arithmetic average of the set of simulation results. The simulation results predict a shift to a higher resonance frequency, when the RO4003 substrate is locally replaced by the RO3003 substrate. This agrees with the fact that material of lower dielectric density is added to the structure, such that the overall antenna becomes electrically smaller. This is also confirmed by the measurement results in Fig. 7. Closer investigation of the simulation results reveals that the mutual correspondence between the different solvers is not perfect. The accuracy for the simulated center frequencies is comparable for all solvers and is generally better than 3.8%. Possible explanations for the observed deviations are the differences in feed model used and imperfections in the realizations. Namely, air gaps between RO3003 and RO4003 generated during fabrication give a resonance shift towards the higher frequencies for the patch on the inhomogeneous substrate. Also, the coax-to-microstrip transition realized by soldering the 50 Ohm SMA connector causes a feeding line discontinuity. This discontinuity moves the measured resonance of the patch on the homogeneous substrate to lower frequencies by adding some capacitive and inductive parasitics. During simulations, ports are actually exited using a calibration process that removes any undesired reactive effects of the mode mismatch at the port boundary. In the case of measurements, a connector characterization with a following de-embedding from the measurements has to be executed in order to minimize the differences between the antenna model and its practical realization [63].

It is very important to point out that, considering the FcD values, the simulation results have a relatively small dispersion. The maximum deviation of 1.58 %, observed for the antenna on the inhomogeneous substrate, proves the good agreement for all software packages.

4.3.2 UWB antenna

The return loss simulated in between 2 and 9 GHz (50 Ohm port reference) is presented in Fig. 10. The IE-based solvers show a very good agreement. Solely, the FEKO result has a slight shift to higher frequencies. This difference is probably due to the different modeling of the feed. For both HFSS and CST MWS, the use of symmetry planes reduced the calculation time. The central frequencies (Fc) and bandwidths at S11 < - 10 dB are predicted with a tolerance up to 7% (Table 3). Having a non-resonant nature the UWB antenna does not have a clearly defined resonance. Therefore, the estimated bandwidth (at S11 = -10 dB) deviation about the mean may be more indicative. This BW deviation lays within 0.01% for all solvers, which is remarkably low. It shows that the main difference lies in the estimation of the border frequencies for the working band.
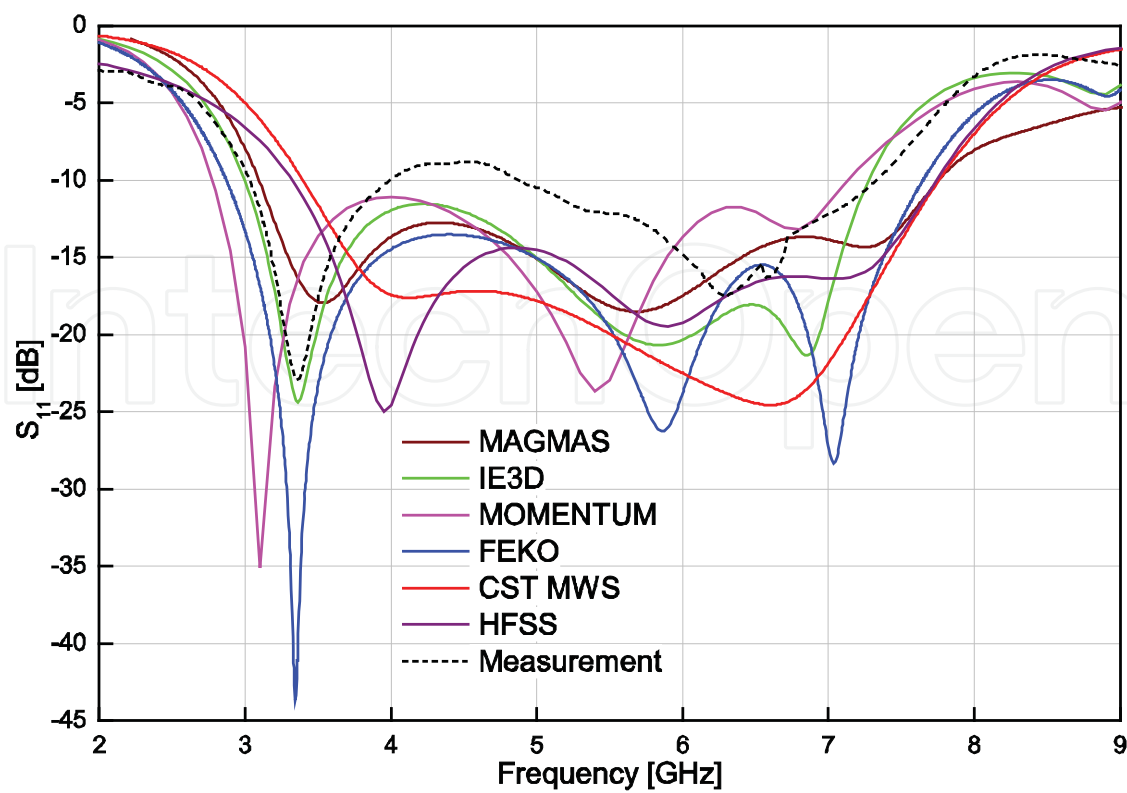
Fig. 10. Simulation and measurement results for UWB monopole antenna topology.

Software Package	Fmin (GHz)	Fmax (GHz)	Fc (GHz)	Fc-shift (%)	BW (GHz)	FcD (%)
MAGMAS	3.11	7.74	5.425	4.73	4.63	2.25
IE3D	3.0	7.27	5.135	-0.87	4.27	-3.22
FEKO	2.87	7.648	5.259	1.53	4.778	-0.88
MOMENTUM	2.77	7.13	4.95	-4.44	4.36	-6.71
HFSS	3.34	7.635	5.488	5.94	4.295	3.42
CST MWS	3.4	7.757	5.579	7.69	4.357	5.14
Measurement	3.03	7.33	5.18	0.0	4.3	-2.37

Table 3. Nominal frequency values for UWB antenna at -10 dB power level.

4.3.3 Folded monopole antenna for GSM applications

The results for the GSM antenna are given in Fig. 11. In the figure, nine results are given, eight calculations and a measurement. Six calculations have been performed at the Katholieke Universiteit Leuven, Belgium, with the several solvers available there. One calculation has been performed at IMST, Germany, with their Empire software tool, and one calculation has been performed at the University of Sienna, Italy, with CST Microwave Studio. The measurement was also performed at the Katholieke Universiteit Leuven.

These results reveal that the solvers really differ, for example concerning the location of the predicted resonant frequencies. It is seen that the curves of all MoM-based solvers agree quite well for the lower resonance. FEKO outlines the middle resonance dissimilar to other solvers, completely merging it with the higher resonance. Among the IE-based software packages, the -5 dB power level in the lower GSM band (900 MHz) was attained by IE3D only, see Table 4. In case the -5 dB criterium was not reached NA is used in Table 4. The volumetric mesh refinement available in CST MWS and Ansoft HFSS helped to uncover the low band resonance. HFSS like CST MWS shows a resonance shift to higher frequencies.
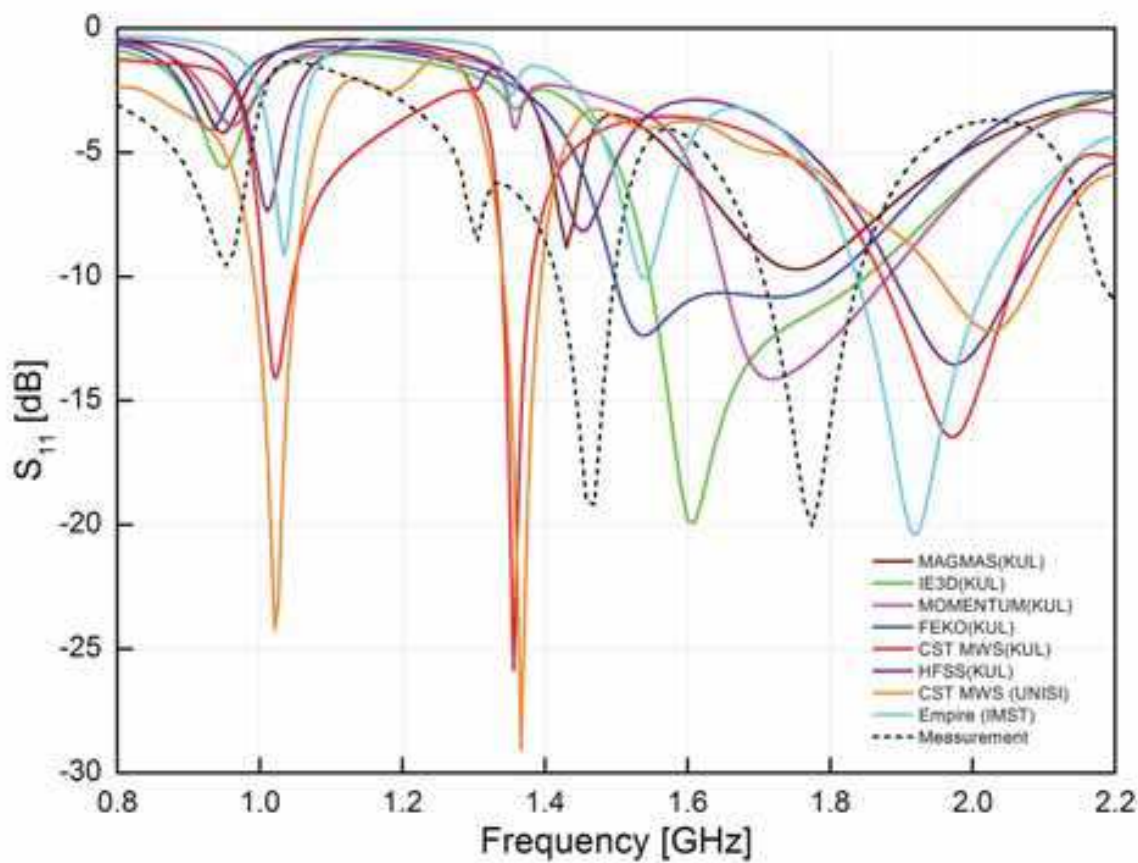

Fig. 11. Simulations and measurement for CPW-fed GSM antenna integrated on a test PCB.

Software Package	1st resonance					
	Fmin (GHz)	Fmax (GHz)	Fc (GHz)	Fc-shift (%)	BW (GHz)	FcD1 (%)
MAGMAS	NA	NA	NA	NA	NA	NA
IE3D	0.932	0.963	0.948	1.45	0.031	-5.80
FEKO	NA	NA	NA	NA	NA	NA
MOMENTUM	NA	NA	NA	NA	NA	NA
HFSS	0.99	1.029	1.01	8.08	0.039	0.36
CST MWS	0.986	1.135	1.061	13.54	0.149	5.43
Measurement	0.882	0.986	0.934	0.0	0.104	-7.14

Software Package	2nd resonance					
	Fmin (GHz)	Fmax (GHz)	Fc (GHz)	Fc-shift (%)	BW (GHz)	FcD2 (%)
MAGMAS	1.404	1.457	1.431	1.96	0.053	0.53
IE3D	NA	NA	NA	NA	NA	NA
FEKO	NA	NA	NA	NA	NA	NA
MOMENTUM	NA	NA	NA	NA	NA	NA
HFSS	1.41	1.505	1.458	3.88	0.095	2.42
CST MWS	1.325	1.437	1.381	-1.57	0.112	-2.95
Measurement	1.271	1.535	1.403	0.0	0.264	-1.41

Software Package	3rd resonance					
	Fmin (GHz)	Fmax (GHz)	Fc (GHz)	Fc-shift (%)	BW (GHz)	FcD3 (%)
MAGMAS	1.577	1.986	1.782	0.39	0.409	-2.75
IE3D	1.493	2.04	1.767	-0.45	0.547	-3.57
FEKO	1.44	1.982	1.711	-3.58	0.542	-6.6
MOMENTUM	1.596	2.033	1.815	2.25	0.437	-0.95
HFSS	1.77	2.19	1.98	11.58	0.42	8.09
CST MWS	1.737	2.138	1.938	9.19	0.401	5.77
Measurement	1.622	1.927	1.775	0.0	0.305	-3.13

Table 4. Nominal frequency values for GSM antenna at -5 dB power level.

4.4 Discussion of the results

The differences are small for the reference antenna. All solvers predict the correct resonant frequency and bandwidth within a small tolerance. The differences are acceptable for the UWB antenna. Also here, the bandwidth is very well predicted by all solvers. For the GSM antenna however, the differences are considerable and not really acceptable. There are several possible causes for this discrepancy. In the following sections, all of them are discussed.

4.4.1 Validity of the input

For the calculations performed at the Katholieke Universiteit Leuven, the input was submitted to and in most cases indeed checked by the technical team of the software vendor responsible for the tool. In some cases, small improvements were suggested and then taken into account. In other cases, an upgrade of the version of the software yielded a slightly different result. For the calculations performed at the other two locations, this check was not performed. Interesting to see is that the two CST calculations are in quite good agreement.

The main conclusion however is that, as far as we can tell, the "quality of the input" is not the cause of the discrepancies.

4.4.2 Meshing

It is well known that the mesh quality and resolution are key factors in the accuracy of any solver. In the case of the GSM antenna for example, the electromagnetic coupling between nearby segments may differ considerably due to the specific meshing used, especially in the meandering parts of the low band monopole and matching circuit. The question is whether the meshes used are adequate. This issue was investigated in the following way. First, simulations were done using standard mesh settings. Second, a convergence study was performed in terms of the resolution of the meshes (see Fig. 12). The high resolution meshes and the lower resolution meshes in practice showed nearly the same results, ensuring that convergence was reached. Third, for each software package, as already mentioned in the previous section, the meshing scheme was submitted to and checked by the software vendor. The general conclusion is that, as far as we can tell, the meshing as used to produce the results shown does not cause the discrepancies.
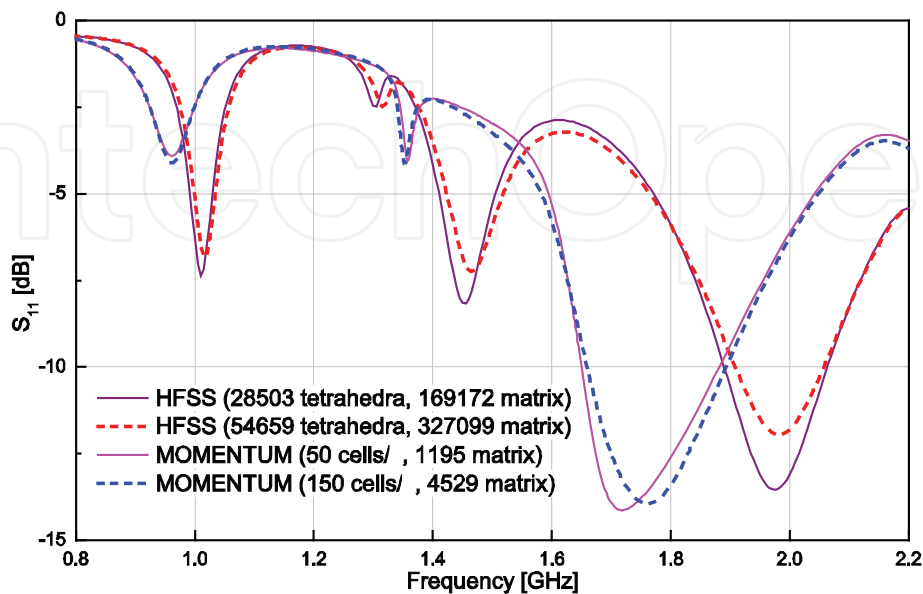

Fig. 12. Solvers convergence for GSM antenna simulation.

4.4.3 Modeling of losses

The importance of taking into account the substrate losses, especially for a lossy material like FR4 (tanδ = 0.02), is obvious. The effect for the GSM and UWB antennas is illustrated in Fig. 13. At the same time, it is known that solvers sometimes tend to show difficulties in accurately modeling losses. This may explain some of the discrepancy between the solvers. It is important to point out that the PCB manufacturing process, although it does not provide adequate uniformity of losses and dielectric constant over the substrates, is not the cause of the discrepancy between the solvers. It could explain some of the discrepancy between the solvers on the one hand, and the measurement on the other hand.
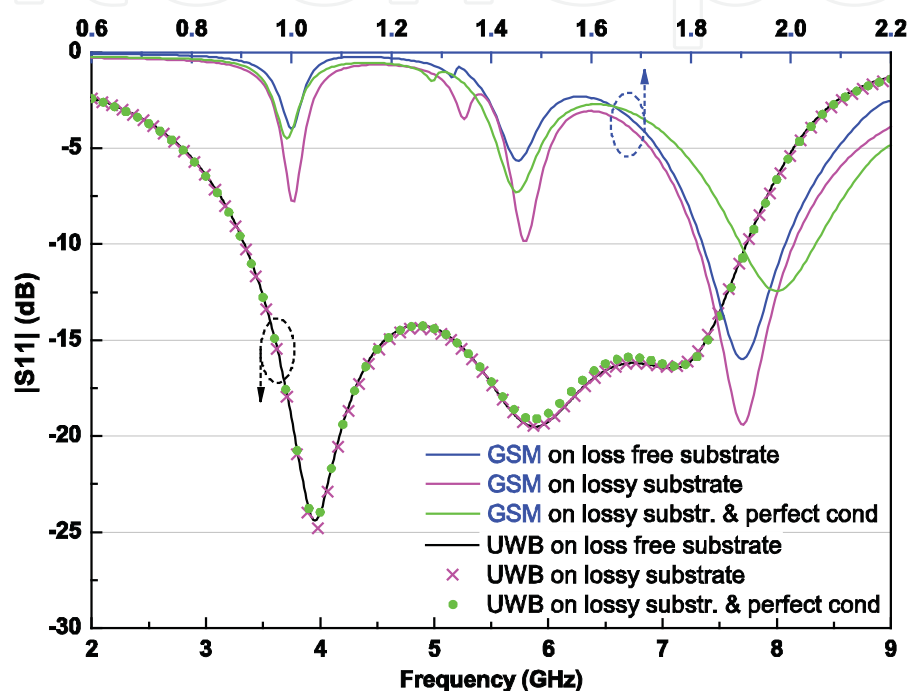
Fig. 13. Simulation results (HFSS) for UWB and GSM antennas considering dielectric and conductor losses.

4.4.4 Implementation of the frequency sweep

Except for MAGMAS all the solvers use fitting functions to model and interpolate the parameters of interest, such as input impedance or S-parameters, in a certain frequency range. Such an adaptive frequency sampling technique automatically selects the sample points. It enables fast and accurate solutions without any a priori knowledge of the parameter of interest. The response is sampled more densely where needed, for example at resonances, to ensure that important details are included. This usually results in run-time savings over discrete frequency sampling. The only observation we want to make is that compared to the standard settings, a quite dense frequency sweep had to be set for HFSS in order not to miss any resonance. Although CST does not need this precaution, its predictions for high-Q resonant antennas are less accurate and slower. The use of the built in auto regressive (AR) filter in CST MWS leads to a faster convergence and helps to avoid the typical ripples, sometimes observed in the more attenuated zones.

4.4.5 Finite or infinite layer structures

Although all MoM solvers used an infinite substrate in the simulations, FEKO and IE3D are able to model finite substrates. Both finite and infinite substrate models have their advantages and drawbacks. Finite substrate models are supposed to be able to include the effects at the edges. However, they enforce the boundary conditions on the top and bottom surfaces of the substrate in a numerical way, in this way losing accuracy on these surfaces. Infinite substrate models enforce the boundary condition on the top and bottom surfaces analytically, and thus rigorously. However, they neglect the edge effects of the finite substrates. A comparison of MoM-based simulation results for both the finite and infinite substrate model is depicted in Fig. 14. The differences are considerable, and the conclusion is clear. Accurate modeling of the finiteness of a layer structure is necessary. Since this was not done for the MoM solvers in Fig. 11, this may explain part of the discrepancy. The non-MoM solvers have another issue. They use a box of finite dimensions to contain the structure. However, from literature, it is well-known that the boundary conditions used on the surface of this box nowadays are of high quality, provided that the box is large enough.
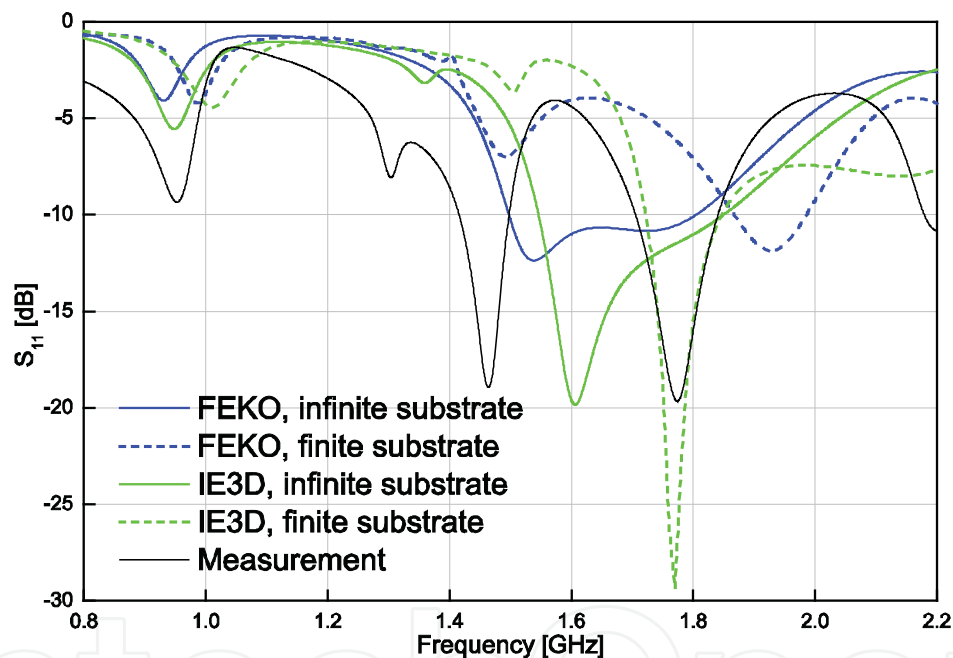

Fig. 14. Simulation results of GSM antenna for both finite and infinite substrate models.

4.4.6 Excitation of the slotline mode in the CPW

The topology is clearly not symmetric with respect to the CPW. In particular, the signal line of the GSM antenna has a meandered matching line which is short circuited to only one ground plane (GP2 in Fig. 5). This asymmetry may give rise to a radiating slotline mode. In practice, the slotline mode is suppressed by connecting the two ground planes of the feeding line with air bridges [64], [65]. The ground planes on the test PCB are connected only at the side of the SMA connector. Inevitably, the slotline mode will appear along with the coplanar mode at the antenna side. The vector E-field plot in Fig. 15a shows the asymmetric slotline mode launched by a lumped port in HFSS, whereas the use of the air bridge in Fig. 15b suppresses the parasitic slotline mode and gives rise to the symmetric CPW mode. Does this

contribute to the observed discrepancy? In theory, it should not. The reason is that as long as a unique and identical topology is inserted in several solvers, the user has the theoretical right to expect identical output. However, it is a fact that the presented EM solvers use different theoretical techniques to derive the scattering parameters of CPW fed structures. It is clear that this may considerably contribute to the simulation results diversity. This is also clearly confirmed by simulations, which exhibit a significant difference when the transversal air bridge is added at the end of the CPW line (Fig. 16). The air bridge was modeled as a bond wire whose ends were soldered to both ground planes in order to equalize their potentials. The position and length of the bond wires have a big influence on the resonant frequency of the two lowest resonances. Normally, the power leaking to the slotline mode can be identified as the main contribution to the losses of the CPW feeding line [66].
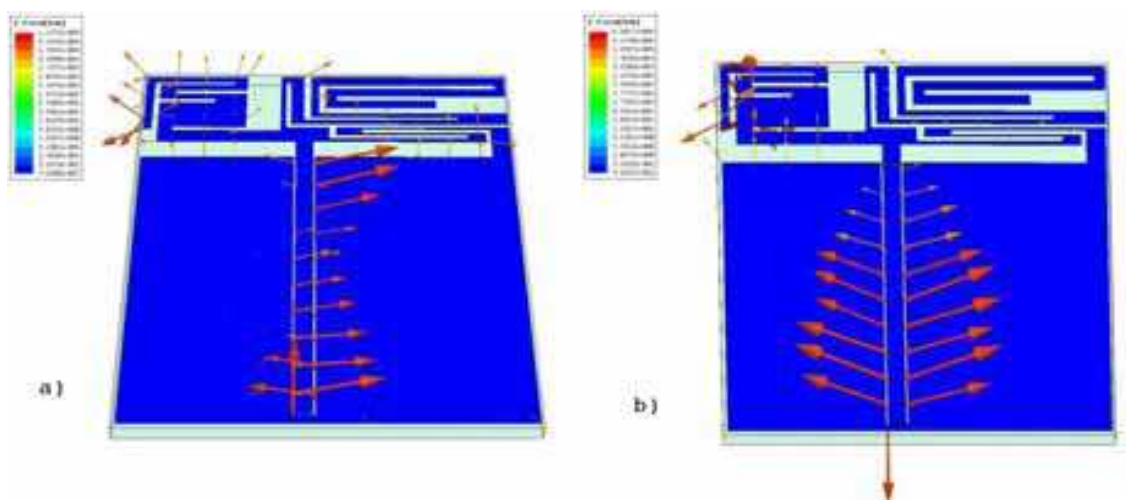
Fig. 15. E-field plot for GSM antenna simulated at 1.8 GHz in HFSS: a) without the air bridge, b) with the air bridge at the end of the CPW.
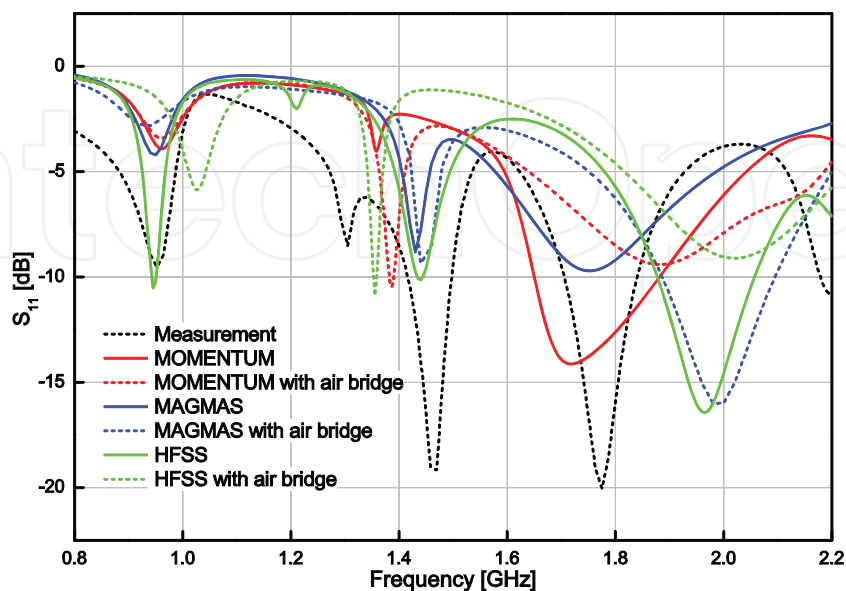

Fig. 16. Simulation results for GSM antenna with air bridge placed at the end of the CPW.

4.4.7 Modeling of the feed

In the case of small planar antennas, the issue of the modeling of the antenna feed is really essential. Since a different feed topology may result in completely different performance, a proper choice of the feed model is absolutely crucial. The basic rule is that the model to select has to correspond as closely as possible to the actual feed topology that is going to be used later in practice.

Most software packages offer several feed topologies. In general, a distinction can be made between the "local" feeds and the "transmission line" feeds. The local feed in essence consists of a localized current or voltage source, possibly with inner impedance. During the simulation, an imposed current or voltage is applied to the structure and its effect is analyzed. It is evident that this feeding topology is really a local one, not able to incorporate with high accuracy the effect of any transmission line that maybe in practice is feeding the structure. The transmission line feed assumes a transmission line (which can be very general, involving multiple conductors, waveguides, etc.) supporting incoming waves exciting the antenna structure. If necessary, the software calculates the eigenmodes of the two-dimensional feed face region. Any actual excitation may be written as a superposition of the eigenmodes. In many software packages there is also a relation between the "local" feeds and the "transmission line" feeds. A transmission line feed in many cases is derived from a local feed by a so-called de-embedding procedure [67].

Which feed is chosen best depends on the structure that has to be modeled. If it concerns an antenna embedded within a mobile device, not fed by a long coaxial cable, the discrete port may be the most appropriate. If it concerns a small antenna embedded within a PCB, fed by a microstrip line, the transmission line feed is probably the proper choice.

Also, in between software packages, there are significant differences in the possible range of models offered for the feed of the antenna. This will certainly contribute to any discrepancy. The question is how much? Let us concentrate on the case of the GSM antenna. The fabricated structure has a coax to coplanar waveguide transition and utilizes the right-angle SMA connector (R125680000 by Radial®) in the measurement setup. Such a feeding setup inevitably induces unwanted parasitics, which affect the characteristics of the antenna.

It has to be emphasized that only in the Empire simulation the connector feeding the fabricated structure was modeled in more detail. There a coaxial feed model was used similar to this connector. The concentrated port impedance of this coaxial feed was set to 50 Ω. The other simulations used the implemented feeding techniques embedded within the solvers, which is the standard practice in most designs reported in literature. These simulations with Empire showed that the connector feeding the antenna has a strong influence on the results.

This puts the antenna design community in a tough position. If the mere presence of the connector indeed alters the results beyond expectation for this type of complicated antenna, this means that it has to be taken into account always in the analysis. This is not possible up to now with the IE solvers and would lead to much larger calculation times for HFSS and CST. Even the slightest difference between the feed model defined by the software user and the actual setup can lead to radical differences in results [68]. Two different feed models were studied in MAGMAS (Fig. 17). Both of them apply the horizontal current source, which consist of a user-defined electric current imposed on a so called active patch. The first topology has the active patch placed between the antenna feeding point and its ground

plane (Fig. 17a). The second topology fully models the CPW feed with the active patch set on the actual feeding point of the SMA connector in the measurements setup (Fig. 17b). Simulated S11 results highlight the substantial importance of the feed modeling (Fig. 18).
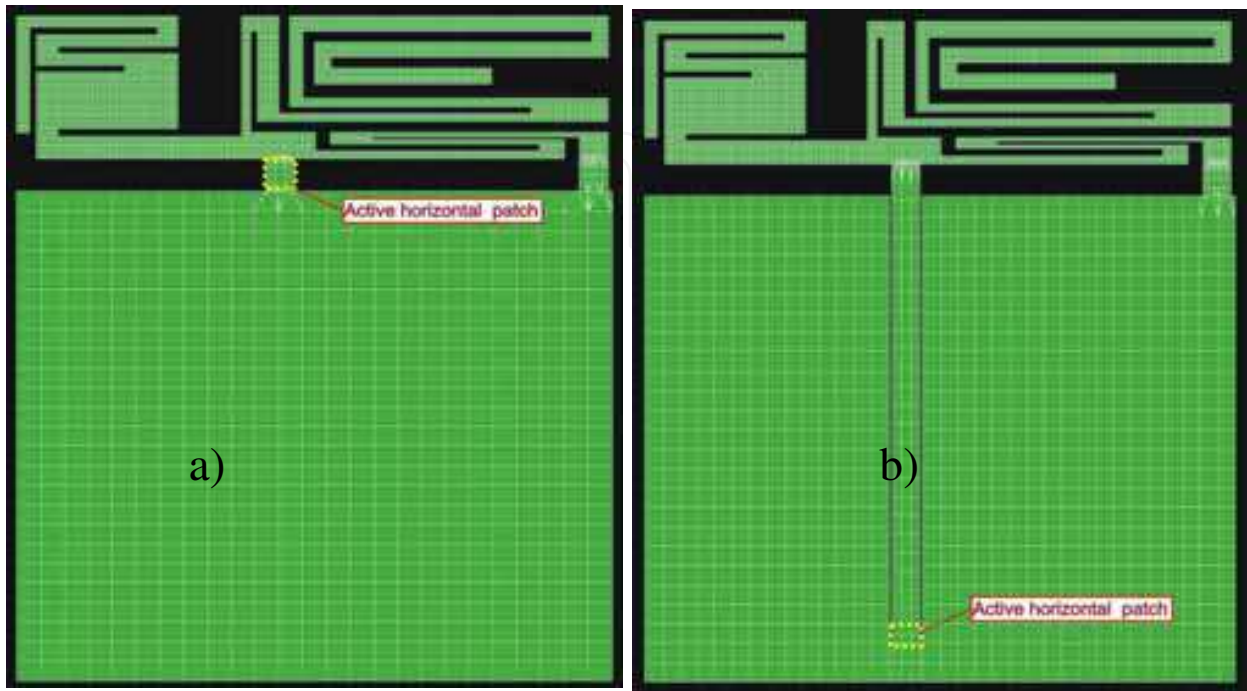

Fig. 17. Different feed topologies for GSM antenna analysed in MAGMAS and HFSS: a) simplified model with localized active patch; b) more advanced CPW feed model.
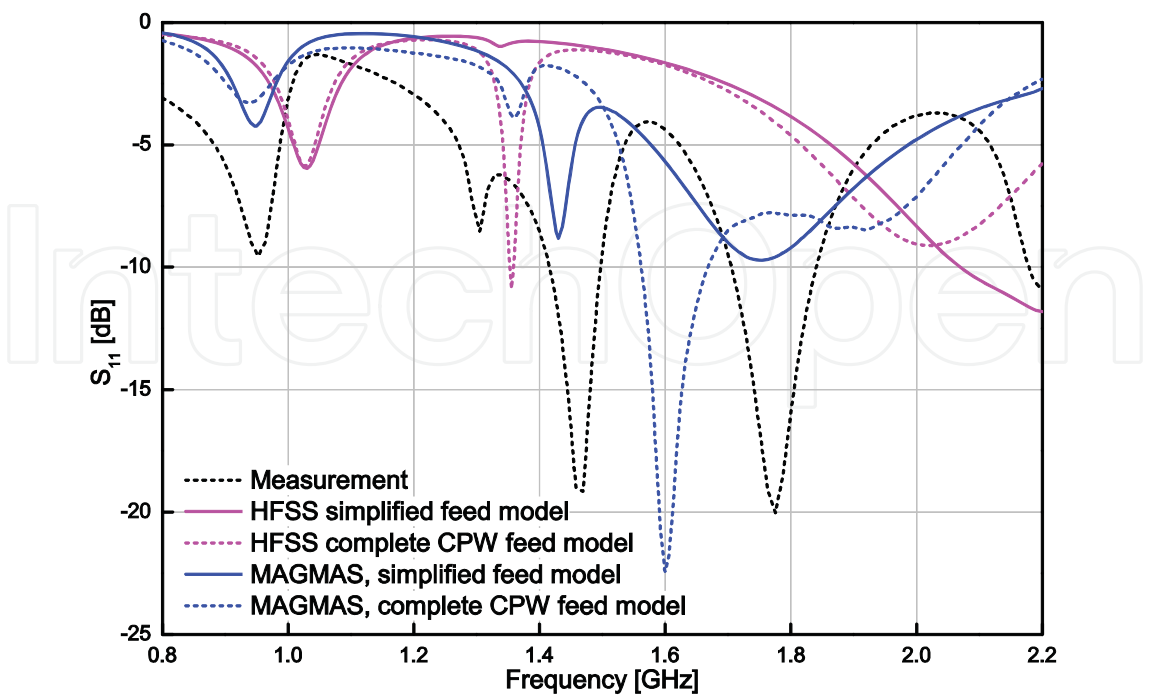

Fig. 18. Simulation results of GSM antenna for different feeds.

4.5 Calculation speed

The simulation time per frequency point (SPFP) and total simulation time (TST) in seconds are presented with the number of unknowns (NU) employed for every structure in Table 5. Several computers with different specifications and operation systems were used to run all the simulations. Table 6 offers an overview of the software tools and the computers used. For the UWB and both square patch antennas a symmetry plane was applied in HFSS and CST MWS. If the symmetry plane is specified, the calculation domain is cut by half. This size reduction of the problem helps to reduce the solution time. It is noticeable, that IE3D performs remarkably fast among the MoM-based solvers. It is only fair to mention that this was only attained after the installation of a "solver version" dedicated to the specific Win64 architecture of the processor used. This IE3D version was provided by the Zeland company during our discussion phase with the software vendors. Without installing the dedicated software version, the times were comparable to the times of the other MoM software packages. It also has to be pointed out that the number of frequency points used was not the same for all software packages, explaining why, comparing two packages, a SPFP time can be lower, while the TST is higher In order to compare the inherent speed of packages, the SPFP times are more appropriate. For the GSM antenna, since we have complete control over its source code, the MAGMAS results were calculated as reference results. They were consequently obtained with a very high number of unknowns. This explains the large calculation times for this topology.

Antenna type		Software package					
		MAGMAS	IE3D	FEKO	Momentum	CST	HFSS
Patch on an homogeneous substrate	NU	579	403	598	384	353912	60718
	SPFP	3.2	1	9.4	4.3	_	19.7
	TST	132	13	122	65	111	237
Patch on an inhomogeneous substrate	NU	3627	999	13801	NA	353912	73394
	SPFP	55	84	929	NA	_	24.6
	TST	2255	1093	12075	NA	107	296
UWB tapered monopole	NU	1663	1595	1367	1748	673507	68076
	SPFP	19	10	63	31.2	_	32.6
	TST	696	169	1136	375	217	391
GSM folded monopoles	NU	6076	740	3879	1195	1724225	169172
	SPFP	367	5	433	15.2	_	126
	TST	26077	76	6062	350	5664	2144

Table 5. Comparative simulation time for different software packages.

Software package	CPU type	RAM installed	Operation System
MAGMAS 3D	Intel Xeon ™ 2.66 GHz	2 Gb	Linux Fedora Core 6
IE3D ver. 12.22	Intel Xeon ™ 2.8 GHz	4 Gb	Windows XP Professional 2002 SP2
FEKO Suite 5.3	AMD Athlon ™ 64 3800+	3.5 Gb	Linux x86_64 2.6.11.9
ADS 2006A.400 Momentum	2 x AMD Opteron ™ 250 (2.4 GHz) 64 bit	4 Gb	Red Hat Linux 2.4.21-27.ELsmp
CST MWS 2006B.03	Intel Xeon ™ 2.8 GHz	4 Gb	Windows XP Professional 2002 SP2
Ansoft HFSS ver. 10.1	2 x Dual-Core AMD Opteron ™ 285 (2.6 GHz) 64 bit	8 Gb	Windows Server 2003, Standard x64 Edition, SP1
Empire XCcel	2 x Intel Xeon ™ 5472 3 GHz	4 Gb	Linux

Table 6. EM solver versions and computer configurations used for the simulations.

5. Conclusions

Planar antennas have to be designed taking into account many aspects. Not only the flatness and size, but also the weight, the ease of manufacturing and the way of mounting become very important. The reason is that in many cases, they have to be integrated in correspondingly small stand-alone systems. This is why the design of planar antennas has become a critical issue in modern telecom system design. In this chapter, an overview has been given on the use of existing computational techniques and software tools for the analysis and design of planar antennas. The available commercial software tools are based on different electromagnetic simulation techniques. They provide the end-user with an intuitive and clear interface. The benchmarking of a wide range of representative electromagnetic simulation tools was carried out. The results are also compared to measurements of the antennas produced. From the study, important conclusions can be drawn.

- As a reference case, the classical patch antenna can be predicted accurately by all simulation programs. Moreover, while having a more attractive market price, MoM based programs perform the simulations inherently faster. Unlike MoM, FEM and FIT are more "brute force" techniques, inherently able to analyse much more general structures. However, they generally require the inversion of much larger, but sparse matrices. This requires the implementation of dedicated inversion techniques, which makes in many cases FEM and FIT based programs memory intensive. Although the calculation times are not that different at present, dedicated inversion techniques for MoM solvers are nowadays fully in development. This fact maybe will change the picture ...

- A proper mesh generation and a correct feeding model are two crucial issues predetermining the successful simulation in the software packages reviewed. In general, a very neat, adaptive mesh refinement implemented in Ansoft HFSS and as an option in CST MWS allows better handling of a design with difficult electromagnetic coupling between its different parts. Such characteristics pertain to applications in mobile gadgets such as the examined GSM antenna. Having no mesh refinement option, MoM based programs require more careful consideration of the initial meshing. MoM solvers can provide an improvement in simulation results and time using so-called edge meshing features, while avoiding excessive meshing on the bulk of the metal structure.

- The more challenging designs such as the GSM and the small UWB antenna require finite substrate effects such as space and surface wave diffraction from substrate edges to be taken into account. MoM-based solvers show better convergence when a dielectric substrate is infinite because then, it is modeled exploiting Green's functions. The practical trend to miniaturize antennas diminishes the advantage of using MoM-based solvers. Having a small size, finite substrate effects such as diffraction and reflection at the edges become more pronounced. Thus, at present FEM and FIT-based programs inherently are better suited for modeling small sized antennas.

In this chapter characteristics important to the customer such as interface, price/performance ratio, user friendliness, and so forth are not considered. However, they are factors influencing the end user's personal choice. The results shown also suggests that the feeding models as implemented today in the widespread commercial solvers are probably unsatisfactory in the case of small structures with complicated electromagnetic coupling behaviour. The slight grouping of results according to the basic theoretical technique used may also be explained by feed modeling, since the feeds used in the three MoM solvers are more alike then the feeds used in HFSS and CST MWS. The study suggests further that the meshing schemes used in all solvers, certainly those including adaptive meshing refinement, are adequate if used properly.

This leads to the following final guideline. The use of two different solvers, based on different theoretical methods (integral and differential) may provide a means to characterize the quality of simulation results. If the two results are in good agreement, it is reasonable to expect that the results can be trusted. If the two results are in disagreement, a deeper investigation of the structure and its modeling is absolutely necessary.

6. Acknowledgements

Excellence on RF-MEMS, whose activities created the proper environment to complete this work.

7. References

[1] D. B. Davidson,"A review of important recent developments in full-wave CEM for RF and microwave engineering," IEEE 3rd Int. Conf. Comp. Electromagnetics and Its Applications, pp. PS/1-PS/4, Nov. 2004.

[2] C. W. Townbridge and J. K. Sykulski,"Some Key Developments in Computational Electromagnetics and Their Attribution," IEEE Antennas and Propag. Magazine, vol. 42, no. 6, pp. 503 – 508, Apr. 2006

[3] E. K. Miller,"A Selective Survey of Computational Electromagnetics," IEEE Trans Antennas Propag, vol. 36, no. 9, Sept. 1988, pp. 1281 – 1305

[4] F. Peterson, S. L. Ray, and R. Mittra, "Computational methods for electromagnetics", IEEE Press – Oxford University Press, 1998.

[5] R. F. Harrington, "Field Computation by Moment Methods", New York: Macmillan, 1968.

[6] T. K. Sarkar, E. Arvan, and S. Ponnapalli, "Electromagnetic scattering from dielectric bodies", IEEE Trans. Antennas Propag., vol. 37, pp. 673-676, May 1989.

[7] Y. Schols and G. A. E. Vandenbosch, "Separation of horizontal and vertical dependencies in a surface/volume integral equation approach to model quasi 3-D structures in multilayered media ", IEEE Trans. Antennas Propagat., vol. 55, no. 4, pp. 1086-1094, April 2007.

[8] M. Vrancken and G.A.E. Vandenbosch, Hybrid dyadic-mixed-potential and combined spectral-space domain integral-equation analysis of quasi-3-D structures in stratified media, IEEE Trans Microwave Theory Tech, vol 51, pp. 216-225, 2003.

[9] G. A. E. Vandenbosch and S. Mestdagh, "Conceptual topology for the integration of planar and quasi 3D antennas in chip packages", IEEE Trans. Antennas Propagat., Oct. 2008.

[10] P. S. Hall and Y. Hao, "Antennas and propagation for body-centric wireless communications", Artech house, 2006.

[11] G. D. Braaten, R. M. Nelson, M. A. Mohammed, "Electric field integral equations for electromagnetic scattering problems with electrically small and electrically large regions", IEEE Trans Antennas Propag, Vol. 56, No. 1, pp. 142-150, Jan. 2008.

[12] Awadhiya.; P. Barba, ; L. Kempel,; "Finite-element method programming made easy???", IEEE Antennas and Propagation Magazine, vol 45, pp.73 – 79, Aug. 2003.

[13] J. M. Jin, The Finite Element Method in Electromagnetics, second edition, John Willey & Sons, Inc., New York, 2002.

[14] J. L. Volakis, A. Chatterjee, and L. C. Kempel, Finite element method for electromagnetics, IEEE Press, Oxford University Press, 1997.

[15] R. L. Courant, "Variational methods for the solution of problems of equilibrium and vibration," Bulletin of the American Mathematical Society, 5, pp. 1-23, 1943.

[16] S. Ahmed, "Finite-element method for waveguide problems," Electronics Letters, vol. 4, Issue 18, pp.387 – 389, Sept. 1968.

[17] R. Coccioli, T. Itoh, G. Pelosi, P. P. Silvester, "Finite-Element Methods in Microwaves: A Selected Bibliography," IEEE Antennas and Propag. Magazine, vol. 38, Issue 6, pp.34 – 48, Dec. 1996.

[18] K. S. Yee, "Numerical Solution of Initial Boundary Value Problems Involving Maxwell's Equations in Isotropic Media," IEEE Trans on Antennas Propag, vol 14, pp. 302-307, 1966.

[19] Taflove, Computational electrodynamics: the finite difference time domain method, Artech House, 1997.

[20] D. M. Sullivan, "Electromagnetic simulation using the FDTD method", Wiley – IEEE Press., 2000, ISBN 978-0-7803-4747-2.

[21] Empire, Version 4.2, IMST GmbH, http://www.empire.de/main/Empire/en/home.php.

[22] Maurice Weiner, "Electromagnetic analysis using transmission line variables", World Scientific Publishing Company, 2001, ISBN 13: 978-9810244385

[23] T. Weiland, "A discretization method for the solution of Maxwell's equations for six-component fields", Electronics and Communications AEÜ, vol 31, No. 3, 116–120, 1977.

[24] Bossavit and L. Kettunen,"Yee-like schemes on a tetrahedral mesh, with diagonal lumping," Int. J. Numer. Model., vol. 42, pp. 129 – 142, 1999.

[25] M. Celuch-Marcysiak and W. K. Gwarek,"Comparative study of the time-domain methods for the computer aided analysis of microwave circuits," Int. Conf. on Comp. in Electromagnetics., pp. 30-34, Nov. 1991.

[26] Agilent Technologies, EEsof EDA, Momentum, http://eesof.tm.agilent.com/products/momentum_main.html

[27] Zeland Software, Inc., IE3D v. 11.2 user manual, Jan 2006, http://www.zeland.com

[28] P. Ciais, R. Staraj, G. Kossiavas, C. Luxey, "Compact Internal Multiband Antenna for Mobile Phones and WLAN Standards", Electronics Letters, Vol. 40, N°15, pp. 920-921, July 2004.

[29] J. Ollikainen, O. Kivekäs, A. Toropainen and P. Vainikainen, "Internal dual-band patch antenna for mobile phones", Millenium Conference on Antennas & Propagation, Davos, April 2000, CD-ROM SP-444, session 3A9.

[30] J. Villanen, J. Ollikainen, O. Kivekäs and P. Vainikainen, "Coupling Element Based Mobile Terminal Antenna Structures", IEEE Transaction on Antennas and Propagations, Vol. 54, N°7, pp. 2142-2153, July 2006.

[31] M. K. Kärkkäinen, "Meandered Multiband PIFA with Coplanar Parasitic Patches", IEEE Microwave Wireless Components Letters, Vol. 15, N°10, pp. 630-150, April 2004.

[32] M. K. Kärkkäinen, "Meandered Multiband PIFA with Coplanar Parasitic Patches", IEEE Microwave Wireless Components Letters, Vol. 15, N°10, pp. 630-150, April 2004.

[33] Z. Ying, "Some Important Antenna Innovations in the Mobile Terminal Industry in the Last Decade", Antenn 06 Conference, 30th May-1st June, Linköping.

[34] EMSS - EM Software & Systems Ltd, FEKO Suite 5.3 user manual, Jan 2006, http://www.emss.co.za

[35] R. Mittra,"A Look at Some Challenging Problems in Computational Electromagnetics," IEEE Antennas and Propag. Magazine, vol. 46, no. 5, pp. 18 – 32, Oct. 2004.

[36] Ansoft Corporation, HFSS v. 10.1.1 user manual, Jul 2006, http://www.ansoft.com

[37] S-H. Yeh, K-L. Wong, T-W. Chiou and S-T. Fang, "Dual-Band Planar Inverted F Antenna for GSM/DCS Mobile Phones", IEEE Transaction on Antennas and Propagations, Vol. 51, N°5, pp. 1124-1126, May 2003.

[38] Y-S. Shin, B-N. Kim, W-I. Kwak and S-O. Park, "GSM/DCS/IMT-2000 Triple-Band Built-In Antenna for Wireless Terminals", IEEE Antennas and Wireless Propagation Letters, Vol. 3, pp. 104-107, 2004.

[39] K-L. Wong and Y-C. Lin, "Thin Internal Planar Antenna for GSM/DCS/PCS/UMTS Operation in a PDA Phone", Microwave and Optical Technology Letters, Vol. 47, N°5, pp. 423-426, December 2005.

[40] W-I. Kwak, S-O. Park and J-S. Kim, "A Folded Planar Inverted-F Antenna for GSM/DCS/Bluetooth Triple-Band Application", IEEE Antennas and Wireless Propagation Letters, Vol. 5, pp. 18-21, 2006.

[41] P-L. Teng, T-W. Chiou and K-L. Wong, "Planar Inverted-F Antenna with a Bent Meandered Radiating Arm for GSM/DCS Operation", Microwave and Optical Technology Letters, Vol. 38, N°1, pp. 73-75, July 2003.

[42] K-L. Wong, S-W. Su, C-L. Tang and S-H. Yeh, "Internal Shorted Patch Antenna for a UMTS Folder-Type Mobile Phone", IEEE Transaction on Antennas and Propagations, Vol. 53, N°10, pp. 3391-3394, October 2005.

[43] CST GmbH – Computer Simulation Technology, CST Microwave Studio 2006 user manual, 2006, http://www.cst.com

[44] MAGMAS 3D, http://www.esat.kuleuven.be/telemic/antennas/magmas/

[45] G. A. E. Vandenbosch and A. R. Van de Capelle, Mixed-potential integral expression formulation of the electric field in a stratified dielectric medium - application to the case of a probe current source, *IEEE Trans. Antennas Propagat.*, vol. 40, pp. 806-817, July 1992.

[46] F. J. Demuynck, G. A. E. Vandenbosch and A. R. Van de Capelle, The expansion wave concept, part I: efficient calculation of spatial Green's functions in a stratified dielectric medium, *IEEE Trans. Antennas Propagat.*, vol. 46, pp. 397-406, Mar. 1998.

[47] Y. Schols and G. A. E. Vandenbosch, Separation of horizontal and vertical dependencies in a surface/volume integral equation approach to model quasi 3-D structures in multilayered media, *IEEE Trans. Antennas Propagat.*, vol. 55, no. 4, pp. 1086-1094, April 2007.

[48] K. G. Gupta, T. Itoh and A. A. Oliner, "Microwave and RF Education – Past, Present, and Future," IEEE Trans. Microwave Theory Tech., vol. 50, pp. 1006–1014, Mar. 2002.

[49] R. Mittra,"A Look at Some Challenging Problems in Computational Electromagnetics," IEEE Antennas and Propag. Magazine, vol. 46, no. 5, pp. 18 – 32, Oct. 2004.

[50] Vasylchenko, Y. Schols, W. De Raedt, and G. A. E. Vandenbosch, "Quality assessment of computational techniques and software tools for planar antenna analysis", IEEE Antennas Propagat. Magazine, Feb. 2009.

[51] M. Vrancken, Y. Schols, W. Aerts and G.A.E. Vandenbosch, Benchmark of full Maxwell 3-dimensional electromagnetic field solvers on prototype cavity-backed aperture antenna, AEU - Int J of Electronics and Communications, 2006.

[52] M. Vrancken, W. Aerts and G.A.E. Vandenbosch, Benchmark of full Maxwell 3-dimensional electromagnetic field solvers on SOIC8 packaged and interconnected circuit, Int J RF Microwave Comput Aided Eng, vol 16, 143-154, 2006.

[53] D. M. Pozar, S. Duffy and A. Herscovici,"A comparison of commercial software packages for microstrip antenna analysis," IEEE Ant. and Propag. Soc. Int. Symp., vol. 1, pp. 152-155, Jul. 2000.

[54] V. Radonic, V. Cronojevic-Bengin and L. Zivanov,"Comparison of Commercially Available Full-Wave EM Simulation Tools for Microwave Passive Devices," EUROCON 2005 "Computer as a Tool" Int. Conf., vol. 2, pp. 1699-1702, Nov. 2005.

[55] V. Radonic, V. Cronojevic-Bengin, B. Reljic and B. Jokanovic,"Accuracy of EM Simulation Tools in Modeling of Resonant Left-Handed Microstrip Lines," EUROCON 2007 "Computer as a Tool" Int. Conf., pp. 2104-2109, Sept. 2007.

[56] D. B. Davidson, Computational electromagnetics for RF and Microwave Engineering, Cambridge, UK: Cambridge University Press, 2005

[57] M.J. Vaughan, K.Y. Hur and R.C. Compton, Improvement of microstrip patch antenna radiation patterns, IEEE Trans Antennas Propag, vol 42, pp. 882-885, 1994.

[58] J.-G. Yook and L.P.B. Katehi, Micromachined microstrip patch antenna with controlled mutual coupling and surface waves, IEEE Trans Antennas Propag, vol 49, pp. 1282-1289, 2001.

[59] J. R. Verbiest and G.A.E. Vandenbosch, "A Novell Small Size Printed Tapered Monopole Antenna for UWB WBAN", IEEE Antennas and Wireless Propagation Letters, vol 5, pp. 377-379, 2006.

[60] Z. N. Chen, N. Yang, Y. X. Guo, and M. Y. W. Chia, "An investigation into measurement of handset antennas," IEEE Trans. Instrum. Meas., vol. 54, no. 3, pp. 1100-1110, Jun. 2005.

[61] C. Icheln J. Ollikainen and P. Vainikainen,"Reducing the influence of feed cables on small antenna measurements," Electron. Lett., vol. 35, no. 15, pp. 1212-1214, Jul. 1999.

[62] C. Icheln J. Ollikainen and P. Vainikainen, "Effects of RF Absorbers on Measurements of Small Antennas in Small Anechoic Chambers," IEEE AESS Systems Magazine, pp. 17-20, Nov. 2001.

[63] M.A. Goodberlet and J.B. Mead, "Microwave Connector Characterization," IEEE Microwave Magazine, vol. 7, no. 5, pp. 78-83, Oct. 2006.

[64] M. Rittweger, M. Abdo, and I. Wolf, "Full-wave analysis of coplanar discontinuities considering three dimensional bond wires," IEEE MTT-S Dig., pp. 465–468, 1991.

[65] Omar and Y. L. Chow, "A solution of coplanar waveguide with airbridges using complex images," IEEE Trans. Microwave Theory Tech., vol. 40, pp. 2070–2077, Nov. 1992.

[66] E. A. Soliman, P. Pieters, E. Beyne and G. A. E. Vandenbosch, "Suppression of the Parasitic Modes in CPW Discontinuities Using MCM-D Technology – Application to a Novel 3-dB Power Splitter," IEEE Trans. Microwave Theory Tech., vol. 46, pp. 2426–2430, Dec. 1998.

[67] M. Farina and T. Rozzi, "A short-open deembedding technique for method-of-moments based electromagnetic analysis", IEEE Trans. Microwave Theory Tech., vol. 49, pp. 624–628, Apr. 2001.

[68] H. ElKamchouchi and G. Abouelseoud, "Automating the Electromagnetic Simulation Procedure and Its Possible "Fatal" Consequences," IEEE Antennas and Propagation Magazine, vol 49, pp. 133–142, Apr. 2007.

[69] P. Ciais, C. Luxey, A. Diallo, R. Staraj, G. Kossiavas, "Pentaband internal antenna for handset communication devices", Microwave and Optical Technology Letters, Vol. 48, N°8, pp.1509-1512, August 2006.

[70] S. Radiom, H. Aliakbarian, G. A. E. Vandenbosch, and G. Gielen, "An Optimized Small-Size Tapered Monopole Antenna for Pulsed UWB Applications Designed by a Genetic Algorithm", IEE Proc. Microwaves, Antennas Propagat., vol. , no. , pp. -, accepted Oct. 2008.

Microstrip Antennas

Edited by Prof. Nasimuddin Nasimuddin

In the last 40 years, the microstrip antenna has been developed for many communication systems such as radars, sensors, wireless, satellite, broadcasting, ultra-wideband, radio frequency identifications (RFIDs), reader devices etc. The progress in modern wireless communication systems has dramatically increased the demand for microstrip antennas. In this book some recent advances in microstrip antennas are presented.

How to reference

In order to correctly reference this scholarly work, feel free to copy and paste the following:

Guy A. E. Vandenbosch and Alexander Vasylchenko (2011). A Practical Guide to 3D Electromagnetic Software Tools, Microstrip Antennas, Prof. Nasimuddin Nasimuddin (Ed.), ISBN: 978-953-307-247-0, InTech, Available from: http://www.intechopen.com/books/microstrip-antennas/a-practical-guide-to-3d-electromagnetic-software-tools

INTECH
open science | open minds